Development and implementation of high-throughput phenotyping tools for microalgae

by Harvey Bates

Thesis submitted in fulfilment of the requirements for the degree of

Doctor of Philosophy

Under the supervision of

Prof Peter Ralph

Dr. Milán Szabó

Dr. Alonso Zavaleta Fernandez de Cordova

University of Technology Sydney

Faculty of Science (Climate Change Cluster)

November 2020

Certificate of Original Authorship

I Harvey Bates, declare that this thesis, is submitted in fulfilment of the requirements for the award of Doctor of Philosophy, in the Faculty of Science (Climate Change Cluster, C3) at the University of Technology Sydney.

This thesis is wholly my own work unless otherwise referenced or acknowledged. In addition, I certify that all information sources and literature used are indicated in the thesis. This document has not been submitted for qualifications at any other academic institution.

This research is supported by an Australian Government Research Training Program.

Signature:

Production Note:
Signature removed prior to publication.

Date: November 30, 2020

Acknowledgements

I would like to thank my supervisors, Prof Peter Ralph, Dr. Milán Szabó and Dr. Alonso Zavaleta for their support, guidance and encouragement over the past few years. Despite our time-zone and spatial differences it has been great gain your friendship and expertise. If it were not for your encouragement to peruse areas outside of my comfort zone this thesis could not have been formulated.

I would also like to thank the technical staff (including but not limited to Paul Brooks and Scott Allchin) at the Climate Change Cluster for their role in assisting me in the laboratory over the course of my candidature.

Finally, I would like to thank my family for their support during my studies.

Contribution of Authors

Each chapter of this thesis was overseen by Prof Peter Ralph, Dr. Milán Szabó and Dr. Alonso Zavaleta. This includes the formulation of concepts, experiments and reviews/editing of text.

Thesis Format

This thesis is compiled with published, submitted and in preparation manuscripts. An introductory chapter is used to explain concepts and review the current state of literature on the explored topics. Chapters two to four are experimental chapters where instrumentation is developed, tested and novel experiments are carried out. The thesis synthesis is used to explore the broad reach that this research applies to and present concepts that may help to drive future microalgal physiological research.

Nomenclature

Acronyms

ETR_{II}	Absolute electron transport rate of photosystem II
PAR_{II}	Photo absorption rate of photosystem II
PI_{abs}	Performance index (absorption)
R	Correlation coefficient
V_j	Relative variable fluorescence at the J-step
Z	Z-score
3D	Three dimensional
pmf	Proton motive force
A	Ampere
ADC	Analog-to-digital converter
ADP	Adenosine diphosphate
AL	Actinic light
ATP	Adenosine triphosphate
C	Capacitor or capacitance
CEF	Cyclic electron flow
DAQ	Data acquisition device
DC	Direct current
DC-DC	Direct current to direct current

Fd	Ferredoxin
FRR	Fast repetition rate
ID	Inner diameter
IDE	Integrated development environment
IV	Intravenous
LC	Light induction curve
LED	Light emitting diode
LEF	Linear electron flow
LHC	Light harvesting complex
LiPo	Lithium-ion polymer
MC-PAM	Multicolour pulse amplitude modulated fluorometer
$NADP^+$	Nicotinamide adenine dinucleotide phosphate reduced
NADPH	Nicotinamide adenine dinucleotide phosphate hydrogen
ND	Neutral density
OD	Optical density or outer diameter
OD_{875}	Optical density determined at 875 nm
OEC	Oxygen evolving complex
P_{max}	Maximum photosynthetic rate as determined by a PI-Curve
PAM	Pulse Amplitude Modulation
PAR	Photosynthetically active radiation (400 - 700 nm)
PBR	Photobioreactor
PC	Plastocyanin or personal computer
PCB	Printed circuit board

PGI	Plotting graphical interface
Pi	Inorganic Phosphate
PI-Curve	Photosynthesis-irradiance curve
PLA	Polylactic acid
PQ	Plastoquinone
PQ Pool	Plastoquinone pool
PSI	Photosystem I
PSII	Photosystem II
PWM	Pulse width modulation
Q_A	Quinone A
Q_B	Quinone B
qE	Energy dependent quenching
R	Resistance
RB	Red blue
RCII	Reaction center of photosystem II
rETR	Relative electron transport rate
RGB	Red green blue
RPi	Raspberry pi computer
SMD	Surface mount device
SQL	Structural query language
T	Transistor
V	Volt or voltage
VDE	Violaxanthin de-epoxidase

VNC	Virtual network computing

Glossary

$\Delta\Psi$	Electrical potential
ΔpH	Change in pH (proton gradient)
$\phi PSII$	Effective quantum yield of photosystem II
$\phi PSIIQ_A$	Quantum efficiency at the J-step (Q_A only)
σ_λ	Wavelength-dependent functional cross section of photosystem II
$^1O_2$	Singlet oxygen
F_i	Fluorescence intensity at the I-step
F_j	Fluorescence intensity at the J-step
F_m	Maximum fluorescence intensity (equivalent to the P-step)
$F_m^{'}$	Maximum fluorescence intensity under actinic illumination
F_o	Minimum fluorescence intensity (equivalent to the O-step)
F_t	Fluorescence intensity immediately before saturation pulse under actinic illumination or the fluorescence intensity at some time-point
F_v	Variable fluorescence
F_v/F_m	Quantum efficiency of PSII if all reaction centres are open (ϕ_{Po} or ϕ_{po} or $Y(II)_{MAX}$)
FN_{1s}	Normalised fluorescence intensity at one second
FN_t	Normalised fluorescence intensity at a point in time
I_1-level	Maximum fluorescence intensity with an oxidised PQ pool
k	Doubling time of microalgal cells in solution

M_0	Closure rate of PSII
$O - I_1$ rise	Chlorophyll *a* fluorescence rise
V_t	Relative variable fluorescence
$Y(II)$	Effective quantum yield of photosystem II
Bilins	Phycobilisomes
CO_2	Carbon dioxide
FNR	ferredoxin-$NADP^+$ oxidoreductase
JIP-test	Technique for analysing OJIP transients
O_2	Dioxygen
OJIP	Chlorophyll *a* fluorescence technique (fast rise)
P680	Pigment center of photosystem II
$P680^+$	Excited state of the pigment center of photosystem II
P700	Pigment center of photosystem I
PQH_2	Plastoquinol

Constants

ETR_{Factor}	Incident PAR absorbed by photosynthetic antenna and the distribution of energy between PSII and PSI	0.42
L	Avogadro constant	$6.02214076 \times 10^{23}\, mol^{-1}$

LIST OF FIGURES

ABSTRACT

Microalgae are promising candidates for numerous biotechnological applications which may help to create sustainable industries of the future. These include the production of sustainable bio-fuels, bio-degradable plastics and food sources for aquaculture. Due to the scale of microalgal biodiversity there is a clear need for tools to assess microalgal phenotypes in an automated manner. However, currently available tools, such as incubators, are either not suitable for reproducible experiments, due to heterogeneous light exposures and lack of physiological measurements or are too expensive for a high-throughput assessment of genotypes, such as commercial photobioreactors. Therefore, this thesis aims to develop a platform upon which robust, open-source sensors and instruments can be created to propel microalgal research into the high-throughput realm.

This thesis presents a low-cost, open-source, multi-wavelength fast polyphasic rise (OJIP) chlorophyll *a* fluorometer (named *Open-JIP*). This device can assess the fine tuning of photosynthesis in microalgae in a non-invasive and rapid manner. The device is compared to commercial instrumentation to demonstrate its ability to resolve the polyphasic rise of chlorophyll *a* fluorescence and its usefulness as an indicator of stress in microalgae.

The developed fluorometer is then integrated into a 3D printed photobioreactor known as the *Phenobottle*. This instrument can assess photosynthesis in a real-time manner and gives the user the controls to automate environmental variables such as bubbling intensity, light quality/quantity and mixing of microalgal solutions. The devices reproducibility is assessed and a simple guide to its functions are presented.

Using these new devices, a novel probe of photosynthetic electron transport in the microalga *Chlorella vulgaris* is formulated (known as FN_{1s}). This measure-

ment allows for a real-time and non-invasive assessment of photosynthetic electron transport, in terms of the electron turnover rate of the electron transport chain in microalgae at a previously undocumented time resolution. Thus, changes in electron transport can now be observed in a matter of minutes rather than previous methods that took upwards of an hour, and no longer requires complex and expensive instrumentation. This may prove useful for researchers looking to optimise microalgal productivity by maximising photosynthetic productivity.

In the final chapter, the presented phenotyping platform is discussed for its potential applications in other areas of microalgal and terrestrial plant research. Additionally, a novel perspective on conducting microalgal physiological research is presented, which may fast-track biotechnological industries of the future.

CONTENTS

1. INTRODUCTION

1.1 An Introduction to Microalgae

The etymologically correct definition of microalgae can be resolved from the Greek word *mikrós* meaning small and the Latin word *alga*, meaning seaweed. Modern definitions of microalgae include both unicellular and multicellular microscopic organisms that photosynthesise [1]. This definition incorporates both eukaryotes, which are classed by their photosynthetic pigment composition (Green – Chlorophyta, Red – Rhodophyta, Golden and Brown – Ochrophyta) and prokaryotes (Cyanobacteria – Cyanophyta). Such a broad definition gives rise to a large discrepancy in the total number of distinct species; however, some researchers estimate there may be more than 200,000 species of microalgae [2]. As a result of microalgae's large biodiversity they inhabit a wide range of environments including ice, soil, water (fresh, marine and brackish), in symbiosis with lichens, corals and sponges, on bare rocks and within hot springs [1, 3–6].

Some global issues are thought to be alleviated if biotechnological industries involving microalgae can be established. These include the decline in food availability, the need for sustainable fuel sources, the treatment of waste water and the environmental build-up of non-biodegradable plastics [7–10]. Combined with these industrial problems, microalgae are responsible for a considerable amount of carbon dioxide fixation in the world oceans and freshwater environments [11, 12]. These carbon sinks aid in maintaining the carbon cycle and thus is helping to mitigate the effects of anthropogenic climate change [13, 14].

1.2 Microalgae Explored in this Thesis

The microalga *Chlorella vulgaris* (Chlorophyta) is used throughout this thesis. These unicellular eukaryotes are around 2-10 μm in diameter (roughly the size of a red blood cell) [15]. *C. vulgaris* reproduces rapidly (within 24 hours under optimal conditions) by process known as autosporulation where the mother cell houses four daughter cells before rupturing [16]. They are promising candidates for a number of biotechnological applications including; the production of sustainable bio-fuels, the bio-remediation of wastewater and as a food source [17–19].

The cyanobacteria *Synechococcus* (Cyanophyta) is explored in the second chapter of this thesis. This marine microalga (3 μm in diameter) has unique light harvesting complexes (as will be explained in subsequent sections) making them interesting candidates for investigation [20, 21]. They reproduce by a process known as binary fission where deoxyribonucleic acid (DNA) is duplicated before the cell splits in two [22]. *Synechococcus* sp. are ideal candidates for biotechnological applications as they can be genetically modified to enhance the production of valuable bio-compounds such as β-carotene [23].

1.3 Phenotyping Microalgae

1.3.1 Phenotyping Theory

A major focus of microalgal research is the process of searching for microalgal species and strains that exhibit interesting or valuable phenotypes (such as high growth rates, dynamic photosynthesis and the production of valuable bio-compounds) [24]. An organism expresses a *phenotype* at a given moment in time as set of measurable traits. The distinction of time is important, as phenotypes may change over the developmental stage of an organism [25]. This will be discussed in greater detail in the thesis synthesis (Chapter 5). The culmination of all phenotypes (the set of all measurable traits in all environments) is known as an organisms phenome [26].

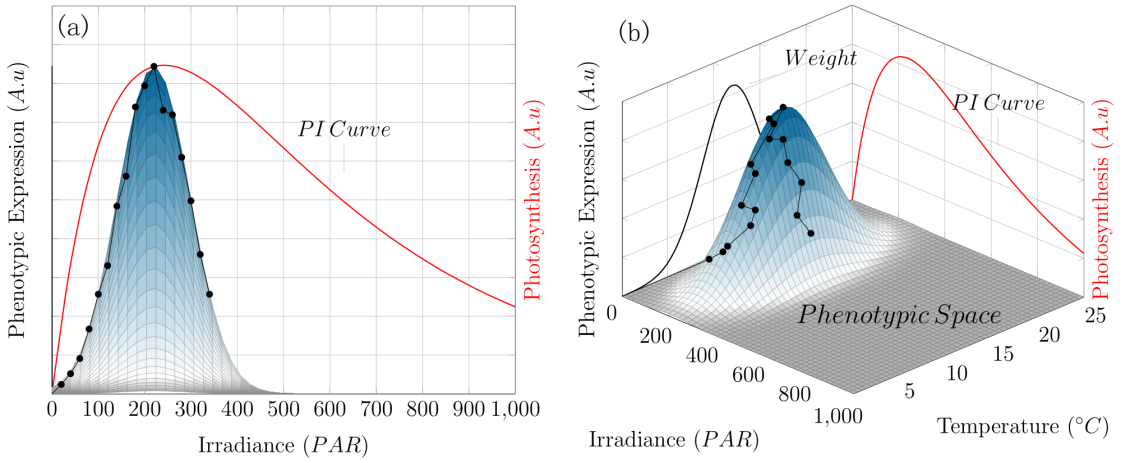

Fig. 1.1: **Theoretical model on the effect of phenotype-environmental interactions**. (a) Demonstrates the effect that various amounts of irradiance have on the expression a phenotype (black line and markers)(in this case the productivity of the microalga). Photosynthetic processes has been modelled to follow a Platt curve (red) with photosynthesis increasing until a saturation point where photo-inhibition becomes a significant factor, resulting in a decline in both photosynthesis and productivity. (b) The same plot is rotated to show both the underlying phenotypic space and another uncontrolled variable (temperature) which is influencing the phenotype-environment interactions. The colormap represents the bivariate influence of environmental variables on the expression of a phenotype; grey - phenotypic space with less that 5 percent expression, white to blue - increasing phenotypic expression. Novel figure with concepts derived in parallel to [27].

It is imperative that environmental conditions that microalgae are phenotyped in are well documented as this creates a clear link between phenotypic expression and the environment. A theoretical model was created to describe the influence of uncontrolled variables on the expression of phenotypes (Figure 1.1). Here photosynthetic performance is plotted against irradiance to demonstrate what is known as a photosynthesis-irradiance curve (PI-Curve) [28]. Concomitantly, the expression of a phenotype is shown, this can represent any observed phenotype, but to simplify this example the productivity (growth) of a microalga can be used here. In Figure 1.1a, as irradiance increases so to does the productivity of the microalgae. Once photosynthesis reaches a maximum value (P_{max}) productivity begins to decrease as photo-inhibition is occurring. From this relationship there is a clear interaction

between the microalgas environment (irradiance) and the observed phenotype (productivity). However, in Figure 1.1b the same plot has been rotated to revel a second environmental variable that may have been overlooked as an additional factor (such as the temperature of the microalgal solution). Now the interaction between the observed phenotype and the organisms environment is not as clear. As temperature fluctuates between cultures, the expression of the microalgas phenotype (productivity) is altered by both irradiance and temperature. This relationship is presented in three dimensions to simplify the example; however, in reality there are practically an infinite number of environmental interactions that are effecting the observed phenotype. Fortunately, the weights that environmental conditions have on expressed phenotypes varies significantly. If environmental variables with known effects on observed phenotypes are controlled (e.g. CO_2 availability, light intensity/quality etc.), then a reasonably accurate phenotype-environment interaction can be formulated.

In addition to mapping environmental variables to expressed phenotypes, it is vital that these interactions are assessed through time [25]. By doing so researchers can create inferences between observed phenotypes and phenotypes that will occur in the future. The technique of probing phenotypes must be as non-invasive as possible to ensure phenotypes are not being altered by the measurement procedure. In addition to this, environmental conditions must be formulated with a high degree of accuracy and broadness to incorporate environmental variables that have a high-probability of effecting observed phenotypes.

1.3.2 Cultivation and Phenotyping of Microalgae

Current cultivations methods for phenotyping microalgae include static or dynamic cultures which are illuminated with light emitting diode (LED) panels or fluorescent tubes. However, these systems succumb to several issues including self-shading (due to stacking of cells when no mixing is present), heterogeneous light exposure between treatments and lack of CO_2 supplementation. However, there are devices that are built to maintain the physiological state of microalgae known as photobioreactors (PBR). Advanced PBR's have controllable light panels, air/CO_2 supplementation,

mixing and some physiological and/or environmental sensors (such as optical density – a measure of microalgal concentration in solution and chlorophyll fluorometers – for photosynthetic assessment). These devices are extremely useful but under utilised in microalgal physiological research as they provide the ability to reproduce experimental data through the control and sensing of environmental conditions. The primary reason PBR's are under utilised is due to the elevated costs of these devices (minimum of US $10,000 ea.). While some researchers may not see this price as an expensive investment, the cost quickly increases as the number of replicates and treatments are considered. As a further deterrent to researchers, the rate at which scientific research is moving does have the ability to make once highly sort after instrumentation obsolete after a short period of time.

1.3.3 High-throughput Phenotyping

Creating a map of environmental interactions with phenotypic expression is a challenging task to accomplish in microalgal research due to the huge diversity of organisms [2]. As a phenotype is a result of an organisms life history, environment and genotype, this undertaking becomes extremely difficult as it requires the assessment of phenotypes in both a large number of genotypes and a large number of environmental conditions [25]. This has resulted in a large number of researchers becoming interested in the process of high-throughput phenotyping their photosynthetic organisms for interesting traits [24, 29]. A high-throughput approach has only recently become adopted by microalgal research [30–32]. However, in plant sciences high-throughput phenotyping is a well developed field of research [29, 33, 34]. The limiting factors in microalgal high-throughput experiments are in the lack of specific instrumentation for these kinds of experimental procedures and the limited customisability of traditional microalgal phenotyping tools.

Conventional phenotyping methods are too labour intensive and slow if one aims to assess a large number of genotypes (Figure 1.2). One aim of high-throughput phenotyping is to speed up the process of searching for valuable phenotypes in microalgae while maintaining sufficient statistical power. Once phenotypes of interest

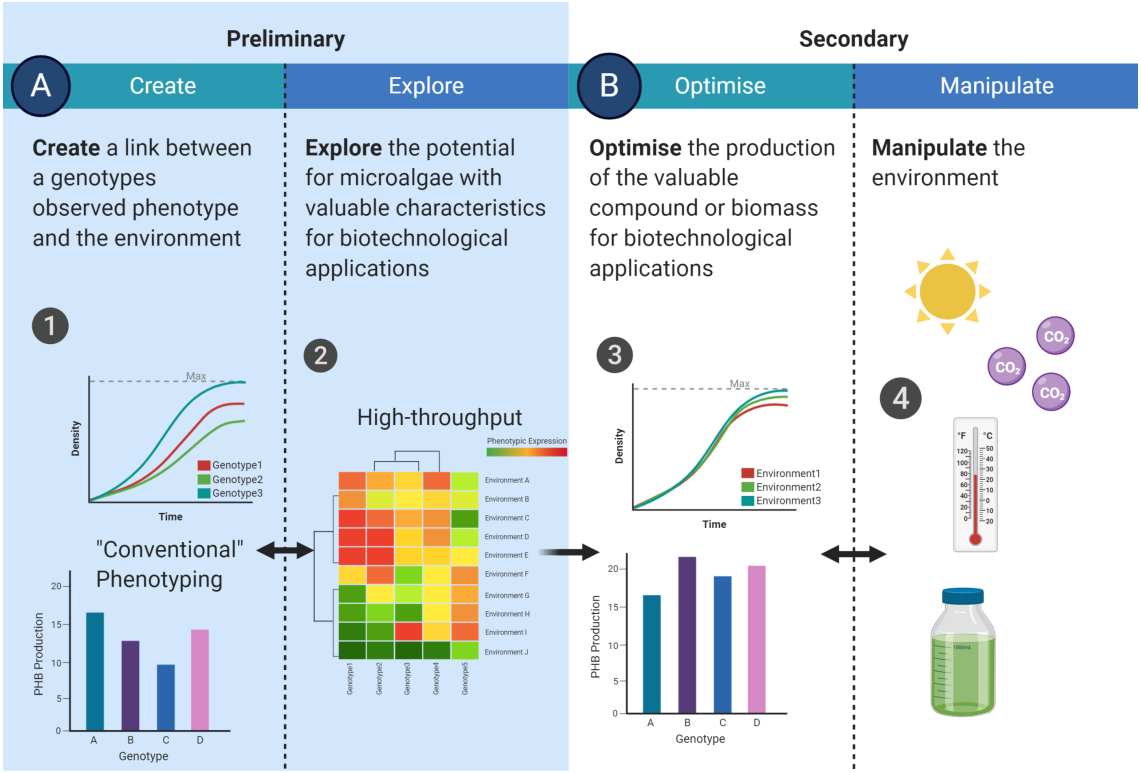

Fig. 1.2: **Phenotyping process involved in microalgal physiological research.** Preliminary (current state of microalgal research) research represents the investigation of genotypes and environmental conditions to resolve interesting phenotypes. Secondary research involves the manipulation of environmental conditions to optimise the expression of a phenotype. Novel figure using example data.

have been explored, then the research focus can switch to the secondary process of optimising the expression of that phenotype. One way this can be done is by optimising the environment upon which that phenotype is expressed (Figure 1.2).

High-throughput phenotyping is commonly performed though the use of imaging, robotics or novel sensors [29]. These devices require very little human interaction to operate, making the suitable for assessing a large number of genotypes autonomously [35]. Ideally, high-throughput phenotyping requires a large number of genotypes, a reasonable number of replicates (to gain statistical power) and as many sensors as possible to resolve as many phenotypic traits as possible [25]. However, due to the extremely high financial investment required for phenotyping facilities this avenue of research is difficult to perform [29]. In microalgal research the abundance of

high-throughput phenotyping tools is rather small, thus this thesis aims to create a platform of instruments for conducting high-throughput research.

1.4 Low-Cost and Open-Source Instrumentation

Throughout this thesis low-cost and open-source instrumentation is presented to phenotype microalgae using non-invasive techniques. Low-cost devices are important in modern day scientific research as these devices allow experimental designs to be expansive without succumbing to excessive costs. This is particularly relevant in high-throughput phenotyping as the current cost of conducting this kind of research is extremely high [25, 29]. From a biological perspective if multiple instruments are used simultaneously then the resolved measurements are representative of the state of the microalgae at a specific point in time. If a single instrument is used then the samples, in most cases, are loaded into the instrument sequentially which may result in greater variations between identical replicates.

The second recurring motif of the thesis is the use of open-source instrumentation. Open-source instrumentation provides users with the knowledge and ability to maintain and upgrade hardware and software [36]. By doing so, one aims to ensure instrumentation in laboratories does not go obsolete. As advancements in scientific understanding of microalgae are formulated then the devices can be modified to adopt the new methods or sensors. The beauty of the presented devices is in the ability for each researcher to customise the device to suit their specific experimental requirements, which can only be achieved if the devices design and instructions are freely available.

1.5 Key Concepts

1.5.1 Photosynthesis in Microalgae

In this dissertation, photosynthetic processes in microalgae are used as a phenotypic trait. As all microalgae have the ability to derive cellular energy through the

process of photosynthesis, the interaction between photosynthetic performance and microalgal productivity is inextricably linked [1]. It is therefore important to provide an introduction to some structures and functions of photosynthesis upon which a baseline understanding of these processes can be used for interpreting subsequent chapters.

Photosynthetic reactions within microalgae can be divided into two phases of energy storage and transportation; 1) the absorption of light by the photosynthetic antenna complexes and the transference of absorbed energy to the functional units of photosynthesis (reactions centres), 2) the stabilisation of excitation energy by secondary processes and the conversion of reducing energy to stable molecules [37]. The first process is known as the *light dependent* reactions of photosynthesis, while the second is known as the *light independent* reactions (does not require excitation energy) [38]. This thesis will refer to the light dependent reactions of photosynthesis, as these process have great potential in the emerging field of high-throughput phenotyping.

Light Absorption by Photosynthetic Antenna

The microalga featured in this work exhibit varying photosynthetic antenna compositions, therefore an introduction to the structure and function of these antenna complexes is provided below. The absorption of a photon by the photosynthetic antenna complexes, located on the thylakoid membrane, triggers a series of reactions [39]. Absorbed energy is passed by neighbouring pigments to the reaction center where it is "trapped" [40] (Figure 1.3). Chlorophyll *a* is the primary photosynthetic pigment found in all eukaryotic photosynthetic organisms [37]. There are a number of chlorophyll molecules that differ structurally due to changes in the composition of their tetrapyrrole ring substituents and the presence or absence of a phytol chain [37]. This results in variances in their wavelength specific absorption [41]. Most forms of chlorophyll have absorption peaks somewhere in the blue-green (450 - 475 nm) and red (630 - 675 nm) wavelengths. However, the pigments (e.g. chlorophyll

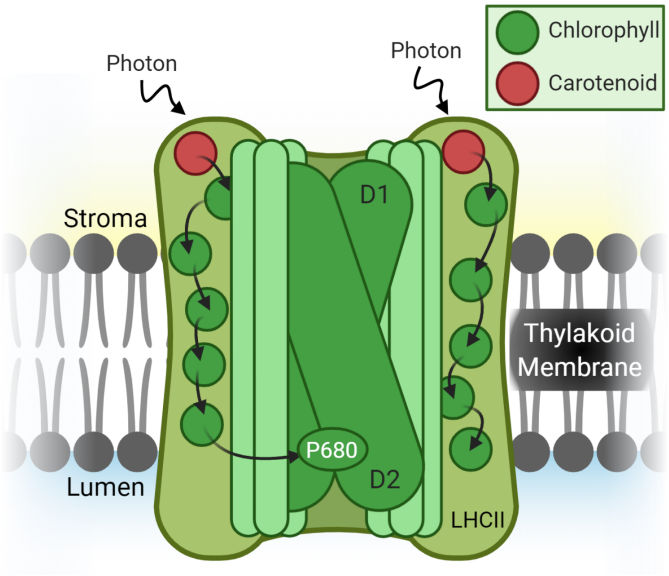

Fig. 1.3: **Simplified diagram of energy transfer from photons to the reaction centre**. The light harvesting complex is located on the thylakoid membrane and houses antenna complexes including chlorophylls (green circles) and carotenoids (red circles). Energy, in the form of photons, hits the photosynthetic antenna resulting in energy transfer to the reaction centre via a special chlorophyll molecule known as P680. Adapted from [37] with modification.

b, *c1-3* and *d*) act to extend the range of absorption that chlorophyll *a* alone cannot absorb [42].

Along with chlorophylls, all microalgae possess carotenoids to broaden their range of wavelength specific absorption (450 - 550 nm) [37]. These carotenoids pass energy to chlorophylls before being funnelled to the primary reaction centres [43] (Figure 1.3). An additional function of carotenoids is their ability to quench the excited chlorophyll's before they form singlet oxygen ($^1O_2$) which can destroy proteins and other structures in the electron transport chain [44].

The green alga used in this work (*C. vulgaris*) has LHC's at two reaction centres known as photosystem I (PSI) and photosystem II (PSII), while the cyanobacteria (*Synechococcus* sp.) possesses an alternative antenna structure known as a phycobilisome. Phycobilisomes are composed of three allophycocyanin disks which are surrounded by rods composed of phycocyanin, phycoerythrocyanin and phycoerythrin disks that radiate outwards [37, 46] (Figure 1.4). Phycobilisomes absorb light

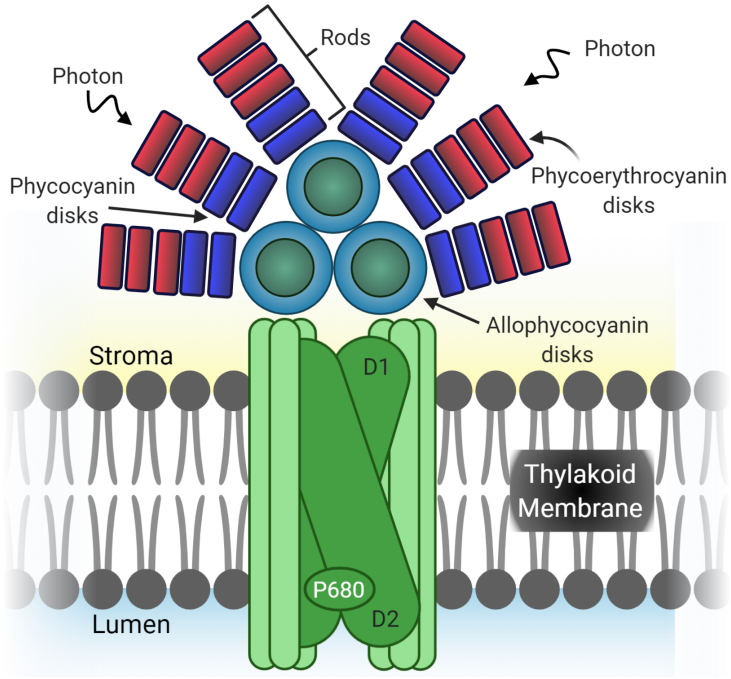

Fig. 1.4: **Phycobilisome structure situated on the thylakoid membrane**. The triangular structure of the phycobilisome optimises light capturing efficiency. High energy absorbing disks (phycoerythrin) are situated furthest from the core and capture light with short wavelengths compared to allophycocyanin disks which are located at the centre of the structure and absorbs low energy (long wavelength) photons. Adapted from [37, 45] with modification.

in the 550 - 650 nm range and funnel excitation energy to the reaction centres of PSI and PSII [47]. This dynamic process allows phycobilisomes to distribute energy between the two photosystems as a response to the microalgae's environment (note that the distribution of energy between PSII and PSI is also possible with LHC's) [47, 48]. The regulation of energy between PSII and PSI by phycobilisomes is known as a state transition, with state one representing a majority of excitation energy being distributed to PSII and state two representing a significant amount of excitation energy being directed to PSI [49].

It is clear that microalgal photosynthetic antenna compositions vary significantly between taxonomic groups. However, the primary function of these antenna structures is similar to terrestrial plants as they all act to capture different wavelengths

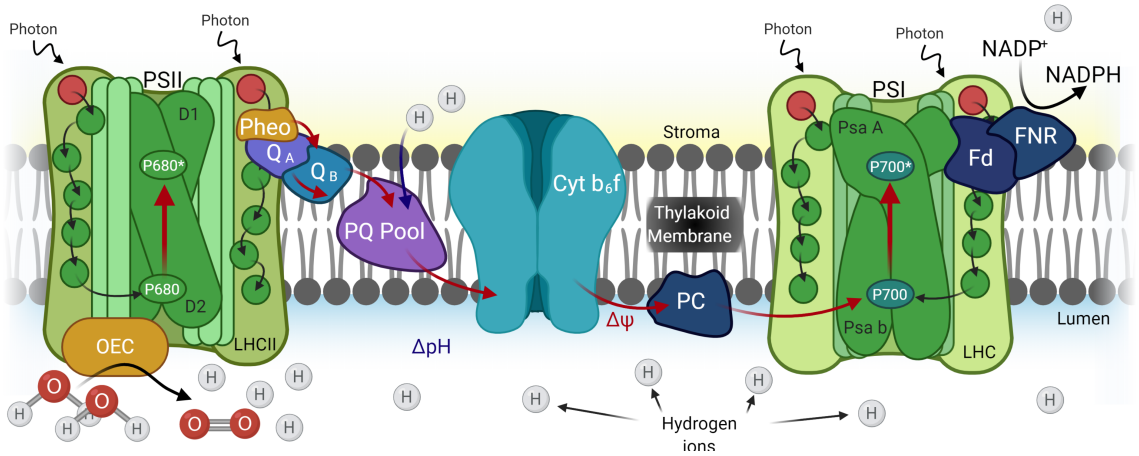

Fig. 1.5: **Representation of linear photosynthetic electron flow**. Red arrows indicate electron transfer ($\Delta\Psi$), blue arrows represent proton translocation (ΔpH) and black arrows represent other forms of energy transfer or processes. Electron transport is initiated at PSII as a result of energy (from photons) being delivered to P680 by the LHC. Adapted from [53] with modification.

and funnel energy to the reactions centres [50]. This results in the initiation of a series of reactions in what is known as the photosynthetic electron transport chain.

Photosynthetic Electron Transport Chain

The main phenotypic trait that can be extracted from photosynthesis is the process of photosynthetic electron transport. This can involve the *linear* flow of electrons (LEF) from PSII to downstream acceptors [51]. These pathways build up a change in electrical potential in the thylakoid membrane ($\Delta\Psi$) due to electron transport and a proton gradient (ΔpH) between the chloroplasts stroma and the thylakoid lumen as a result of proton translocation across the thylakoid membrane [52].

In linear electron flow, when P680 enters its excited state (P680*) the dimer becomes unstable, this can result in electrons being transferred to phenophytin (Pheo) [54]. These electrons are primarily derived from the breaking of two water (H_2O) molecules into their constituents at the oxygen evolving complex (OEC) [53]. In series, from phenophytin, the reduction of electron acceptors includes; the quinones Q_A to Q_B and from Q_B to the plastoquinone pool (PQ pool) [55]. Here plasto-

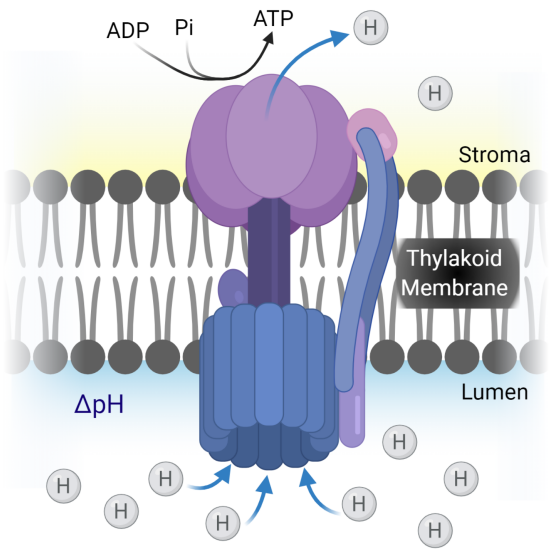

Fig. 1.6: **Representation of ATP synthase activity in photosynthetic organisms**. ADP is combined with Pi to form ATP at ATPase (black arrows) which is activated as a result of proton translocation (blue arrows) out of the the thylakoid lumen across a ΔpH gradient. Adapted from [53] with modification.

quinone (PQ) is reduced to form plastoquinol (PQH_2) which is then oxidised by the cytochrome b_6f complex. This process, depending on the species, generally results in halve the electrons from PQH_2 being passed to plastocyanin (PC) and the other halve to be recycled within the PQ pool to maintain a reduced state. PC acts as an electron carrier between the cytochrome b_6f complex and PSI, where excited P700 dimers carry electrons to ferredoxin (Fd) where ferredoxin-$NADP^+$ oxidoreductase (FNR) converts nicotinamide adenine dinucleotide phosphate ($NADP^+$) into nicotinamide adenine dinucleotide phosphate hydrogen (NADPH).

Concomitantly with electron transport through the electron transport chain a ΔpH gradient begins to build up across the thylakoid membrane [53, 56] (Figure 1.5). The efficiency of proton translocation is known as the proton motive force (*pmf*) and is made up of a proton gradient (ΔpH) and an electrical potential gradient ($\Delta\Psi$). *pmf* acts to drive the conversion of adenosine diphosphate (ADP) into ATP with the addition of an inorganic phosphate (Pi). This conversion occurs at ATP synthase (ATPase) which is located on the thylakoid membrane. ATPase is activated

by a ΔpH gradient between the stroma and the lumen as a direct result of proton translocation (Figure 1.6).

1.5.2 Chlorophyll a fluorescence

As photosynthetic electron transport results in the production of metabolites (ATP, NADPH) for powering other cellular functions in microalgae, the efficiency of this process is highly important. A valuable tool for the high-throughput assessment of photosynthetic phenotypes is through the use of a chlorophyll *a* fluorometer [57]. Chlorophyll *a* fluorescence requires that the photosynthetic sample must be kept in the dark prior to measurement so as to ensure the electron transport chain is completely relaxed (thus creating a reproducible reference state). This method relies upon the application of light to excite PSII [58]. When PSII is in an exited state it becomes unstable and can return to its ground state in three main ways. 1) It can dissipate the energy as heat (non-photochemical quenching), 2) it can transform the energy to reducing power for use in the electron transport chain (photochemistry) or 3) it can be re-emitted as photons (fluorescence) [59] (Figure 1.7). Blockages in the electron transport chain can effect the chlorophyll *a* fluorescence signal. Therefore, by measuring the resulting chlorophyll *a* fluorescence intensity we can derive information regarding the state or efficiency of photosynthesis in microalgae. Information regarding the activity of photo-protection pathways can also be attained from non-photochemical quenching analysis in some methods of conducting chlorophyll *a* fluorescence analysis [60]. The extracted data from chlorophyll *a* fluorescence enables researchers to make informed inferences about the productivity of microalgae at a particular point in time. In my dissertation I have used several methods to measure chlorophyll *a* fluorescence; including, 1) pulse amplitude modulated (PAM) fluorometry and 2) polyphasic rise of chlorophyll *a* fluorescence (OJIP)(Figure 1.8). In Chapter 5 of this thesis I discuss how data extracted from chlorophyll *a* fluorescence could be used as a real-time feedback mechanism in microalgal cultivators to maximise the expression of a valuable phenotype (e.g. productivity).

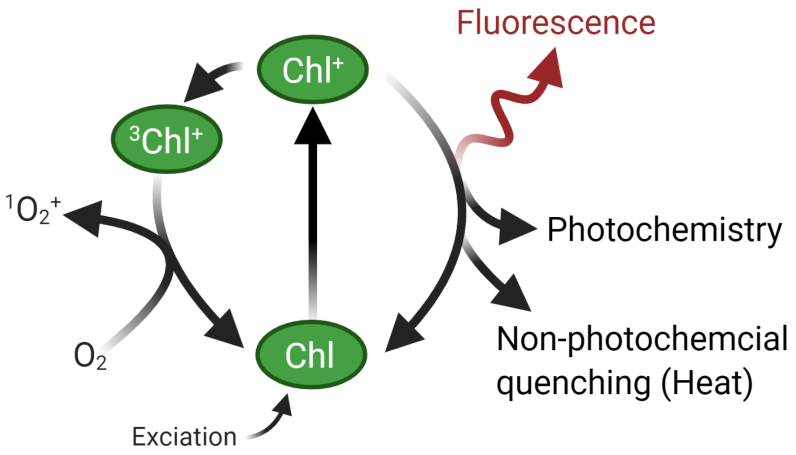

Fig. 1.7: **Energy dissipation pathways of chlorophyll *a* fluorescence.** When chlorophyll is excited there are a multitude of pathways to return to a ground state. It can 1) emit light (a photon) as fluorescence, 2) use the excitation energy to power photochemical reactions or 3) dissipate the energy as heat (non-photochemical quenching). An alternative pathway is through the formation of a triplet state chlorophyll which has the ability to produce a damaging reactive oxygen species ($^1O_2^+$). Adapted from [60] with modification.

Fast Polyphasic Rise (OJIP) Fluorometry

The method of resolving the fast polyphasic rise (OJIP) of chlorophyll *a* fluorescence involves a single saturation pulse (usually around one second in length) of constant actinic light [62] (Figure 1.8a). As the microalga transitions from a dark to light adapted state a number of inflection points appear in the chlorophyll *a* fluorescence signal. These represent different potions of the electron transport chain, due to a blockage of electrons [58, 59]. OJIP fluorescence is an ideal candidate for the process of high-throughput phenotyping microalgae, as the technique is rapid, non-invasive, non-destructive and information rich.

As shown in Figure 1.5 electron transport can occur linearly through a series of reductions and oxidations of electron transporters. The linear nature of this process results in a time series of energy transfer as electrons are accepted by downstream acceptors. As a result of this, each step of the OJIP fluorescence transient is measured at particular time points after the application of the actinic light (O-step - 0.04 ms, J-step 2 ms, I-step - 30 ms) apart from the P-step which is taken as the maxi-

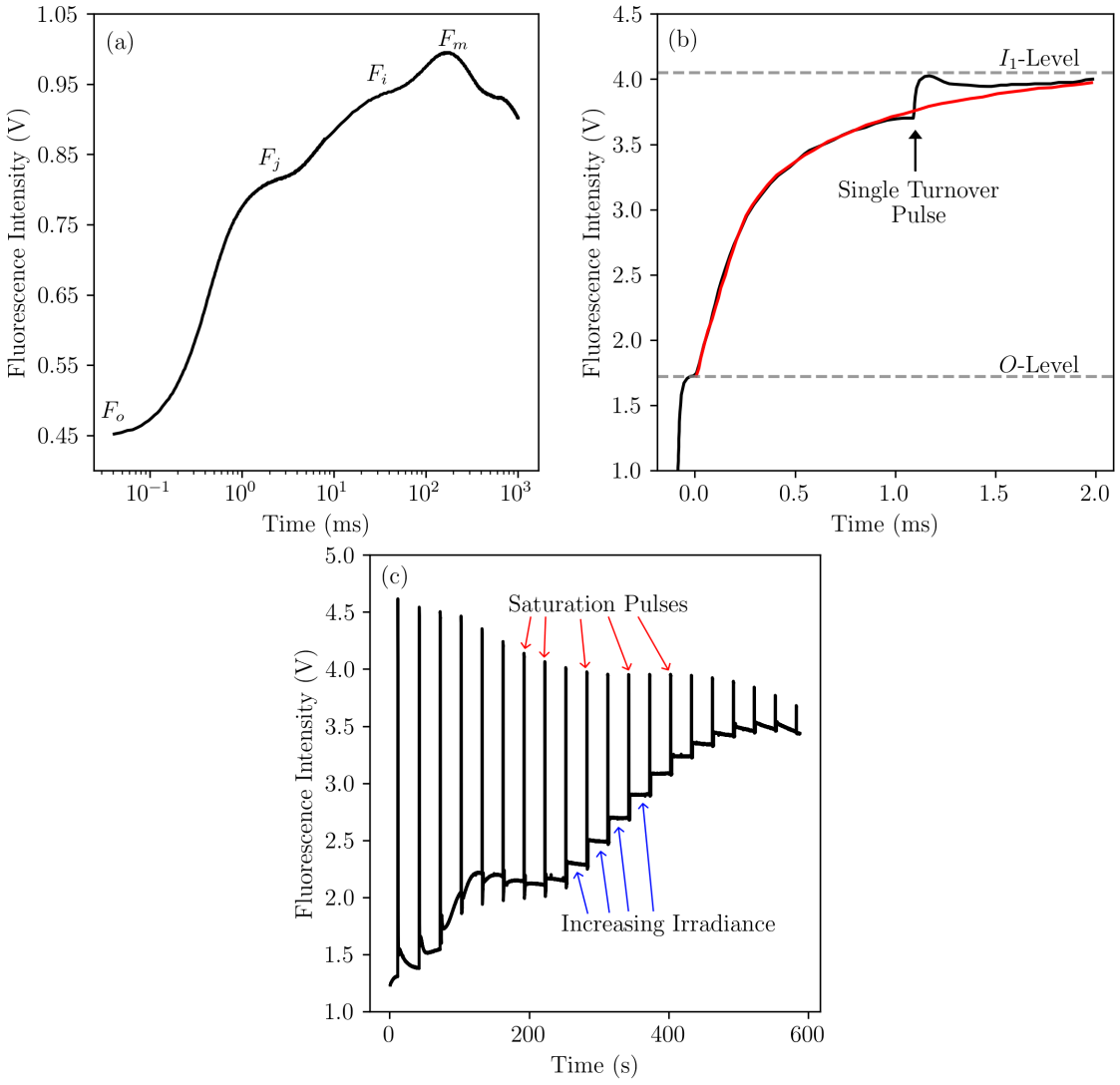

Fig. 1.8: **Three different chlorophyll fluorescence techniques used in this thesis.** (a) OJIP fluorescence, consisting of four main steps; F_o (O-step) - F_j (J-step) - F_i (I-step) - F_m (P-step). (b) PAM fluorescence $O-I_1$ rise, consisting of two main steps; O-level (F_o) and the I_1-level (F_j). The fitted curve (red line) is used to derive the time constant of Q_A reduction. (c) PAM fluorescence light curve analysis. This measurement is much longer (10 minutes) than the previous two examples (milliseconds to seconds). The technique involves increasing actinic light intensity of the fluorometer (at set intervals) while probing variable chlorophyll *a* fluorescence with saturation pulses. Novel figure with data (in part b) from [61].

mum fluorescence intensity (Figure 1.8). These time points represent the reduction of various electron acceptors in the electron transport chain.

The F_o value or O-step, corresponds to the minimum level fluorescence intensity immediately following illumination of the sample (∼0.04 ms). This represents the trapping efficiency of PSII if all reaction centres are open [63]. There is a rapid rise in fluorescence intensity to the first inflection, known as the J-step. The O-J phase (known as the photochemical phase) is formed as a result of the quasi single turnover reduction of Q_A (resulting from a single reduction of all Q_A) by electron donors of PSII [64, 65]. The following two steps (I-step and P-step) are much slower than the initial rise in fluorescence intensity and are temperature sensitive (thus they are known as the thermal phases) [64, 66]. The J-I phase occurs as a result of several processes and is therefore less well characterised when compared to other phases [64]. However, the general consensus is that the J-I phase is a result of Q_B oxidation by the PQ-pool [64]. The I-P phase corresponds to a saturation of electrons on the acceptor side of PSI (ferredoxin) and other photochemical events (Figure 1.5) [67]. Once the electron transport chain is fully saturation with electrons, the P-step (F_m) is visible as the maximum fluorescence intensity.

The OJIP fluorescence transient is commonly interpreted using a algorithm known as the JIP-test [68]. In this analysis fluorescence signals are examined using a model of energy fluxes in bio-membranes to derive several parameters that represent information regarding active reaction centres [68, 69]. One can derive several parameters to predict active reaction center performance. In this work I have used, $F_v = F_m - F_o$ which describes the maximum variable fluorescence of PSII and F_v/F_m - otherwise known as ϕ_{Po}, which describes the maximum quantum efficiency of PSII if all reaction centres were open, M_0 - which indicates the closure rate of PSII under intense illumination or $\phi PSIIQ_A$ - the maximum quantum yield at the J-step (Q_A only) [64, 68, 70]. It is worth noting that these parameters can also be derived from conventional PAM fluorescence procedures as will be explained in the next section [59].

The O-J phase of OJIP fluorescence can also be used to measure the wavelength-dependent functional cross section of PSII (σ_λ) [61] (Figure 1.8b). The technique known as the $O-I_1$ rise differs slightly from conventional OJIP measurements calling

for different nomenclature. A constant monochromatic actinic light is used to probe chlorophyll *a* fluorescence and at ∼1 ms, a single turnover (50 μs in duration) saturation pulse is used to close PSII reaction centres, allowing for the derivation of the I_1-level fluorescence intensity (J-step equivalent). The I_1-level can be derived in under 2 ms and is therefore the maximum fluorescence intensity that can be achieved with an oxidised PQ pool [61].

As the $O-I_1$ rise is wavelength-dependent this measurement is usually calculated at a number of wavelengths within photosynthetically active radiation (PAR) (400 - 700 nm) to explore the microalga's effective antenna size to various colors of light [71]. σ_λ is dependent upon the antenna composition of the microalga, therefore as shown in previous sections, the large variety of photosynthetic antenna complexes leads to a wide range of σ_λ calculations. This parameter is used in chapter 4 of this thesis to optimise the wavelength specific absorption of *C. vulgaris*.

Pulse Amplitude Modulated (PAM) Fluorometry

PAM fluorometers, like OJIP fluorometers, provide a flash of saturating irradiance in order to derive information regarding the state of PSII [72]. These fluorometers can derive the minimum level fluorescence intensity (F_o) by using very low intensity (and low frequency) light to probe PSII without inducing photosynthesis (hence the name amplitude modulation) [72]. Once a saturation pulse is applied to the sample, F_m can be attained as the maximum fluorescence intensity (similar to OJIP fluorescence).

Complementary to OJIP fluorometry, PAM fluorometry has the ability to study the microalgal under both actinic irradiance and saturating irradiance, which cannot be achieved using OJIP alone. PAM fluorescence can be performed by exposing a photosynthetic sample to increasing actinic (light that drives photosynthesis) irradiance intensities at defined intervals (>30 seconds each) while probing photosynthesis at the end of each period by means of a saturation pulse [73] (Figure 1.8). Actinic exposures are designed to be long enough for photosynthesis to be in a steady state

and therefore the resolved parameters are representative of how photosynthesis is functioning at that PAR. Each of the saturations resolves information regarding the effective quantum yield of PSII (ratio of photons used in a light-adapted state) ($\phi PSII$ or $Y(II)$) at the specific actinic irradiance used [61, 74] (Eq. 1.1). This method is demonstrated in Figure 1.8c, whereby 30 second actinic exposures followed by an intense saturation pulse was used to resolve $Y(II)$ at various actinic intensities.

$$Y(II) = \frac{F_m^{'} - F_t}{F_m^{'}} \tag{1.1}$$

Where $F_m^{'}$ is the maximum fluorescence intensity when under actinic light and F_t is the fluorescence intensity immediate before a saturation pule while under actinic light [59, 74]. From this the relative electron transport rate of photosynthesis ($rETR$) can be calculated which is the basis for all subsequent equations demonstrated in chapter 4 of this thesis.

$$rETR = Y(II) \times PAR \times ETR_{Factor} \tag{1.2}$$

Where the PAR is the irradiance applied to the sample in μmol photons m^{-2} s^{-1}. The ETR_{Factor} represents both the amount of incident PAR being absorbed by the photosynthetic antenna and the distribution of energy between PSII and PSI (normally estimated to be 0.42) [75, 76].

1.6 Challenges to be Addressed

Microalgal research has been conducted for over a halve a century, while there has been major advancements in our understanding of these photosynthetic organisms some major challenges remain. Exploring the phenotypic diversity of microalgae has been an area of great interest for researchers (such as through the use of high-throughput phenotyping). This type of research may lead to the discovery of novel strains which exhibit valuable characteristics (e.g. high-growth rates, photosynthetic

plasticity or the production of valuable bio-compounds). However, this has its challenges as there needs to be robust methods to screen phenotypic traits in a rapid and non-invasive manner. Current methods to do this are either too expensive to be a feasible investment for most researchers or non-existent in the current research landscape. Therefore, there is a need for low-cost instrumentation to conduct reproducible high-throughput experiments. Ideally, these devices should have the ability to be upgraded over time to adapt to the ever changing scientific landscape.

A preliminary choice for conducting a high-throughput analysis of microalgal genotypes is through the use of incubators, which provide irradiance and temperature continuity between replicates. These devices also allow for a large number of genotypes to be cultivated simultaneously. However, incubators lack controls over other environmental variables such as CO_2 supplementation for photosynthesis and homogeneity of irradiance. As demonstrated in previous sections, uncontrolled variables can lead to incorrect links between environmental conditions and phenotypic traits. In addition to this, incubators lack physiological sensors which can track phenotypic traits over time. Real-time assessment of traits is vital for a high-throughput assessment of expressed phenotypes and results in incubators being a poor choice for microalgal physiological research.

An alternative to incubators is the use of PBR's, which maintain an array of environmental conditions within pre-programmed regions and have the ability to probe microalgal physiology in real-time. Currently, the use of PBR's are the most practical and robust methods of probing and controlling microalgal physiology. However, as mentioned in a previous sections the price of these devices can quickly result in the formation of large P small n datasets (large number of phenotypes (P) and a small number of replicates (n)) [25]. Therefore, there is a significant need for open-source photobioreactors that can be built to maintain both the environmental continuity between replicates of identical treatments and probe physiology in a non-invasive and autonomous manner. This thesis aims to develop and implement high-throughput phenotyping tools for microalgal research. To design such a platform we first need to develop some low-cost and open-source sensors which can

accurately track phenotypic traits. For this the focus will be on the development of sensors for assessing photophysiology and growth of microalgae. However, as will be discussed in the synthesis, the platform is adaptable to new sensors as the user requires.

The second chapter of this thesis is devoted to the development of a low-cost chlorophyll *a* fluorometer for assessing photo-physiological traits in microalgae (known as *Open-JIP*). This device is key to the subsequent chapters, as it allows microalgae to be screened for photosynthetic phenotypes in a rapid and non-invasive manner. Current chlorophyll *a* fluorometers can be acquired for upwards of $1,000 ea. However, these devices come with very little customisability and for many devices to be acquired, as is required for high-throughput analysis, this cost can increase rapidly. The device developed in this thesis, can be built for under $100 and is capable of measuring photosynthesis accurately in both microalgae and terrestrial plants (two arrangements are presented). Accuracy and repeatability are key factors in the thesis as it is important to design instrumentation that is cost-effective without sacrificing quality. This is addressed in this thesis by using low-cost solutions such as 3D printing structures, considering part costs when designing electronic infrastructure and using high-quality materials (such as optics) when necessary.

The fluorometer which was developed and tested in chapter two is integrated into an in-house made photobioreactor in chapter three. This device is an open-source, customisable instrument that is capable of automatic light control (quality and quantity), mixing of microalgal cultures, bubbling of air and possess an array of physiological sensors. The instrument is named *The Phenobottle* as its primary purpose is to photosynthetically phenotype microalgae. In this chapter the Phenobottle's features are explained and cross examined with commercial instrumentation, along with a benchmark experiment using the green alga *C. vulgaris*. This experiment demonstrates the Phenobottles ability to resolve a time-series assessment of photosynthesis and productivity in microalgae in a non-invasive and autonomous manner. Currently available photobioreactors do not offer enough customisability and low-cost needed to preform high-throughput experiments with microalgae,

therefore making the development of *The Phenobottle* an integral tool for microalgal research.

Microalgal physiological research is lacking a a real-time and accurate probe of photosynthesis. This measurement would give researchers an accurate representation of the state of photosynthesis in microalgae without destroying the sample or altering its physiology. There are some rapid (1 second measurements) methods such as the quantum yield of PSII (termed ϕ_{PO} also known as F_v/F_m) which only assesses the state of specific functional units in the photosynthetic electron transport chain. However, by doing so, a lot of information regarding downstream processes (such as ATP synthase activity) are not monitored. Advanced methods, such as light induction curves (LC), give information regarding the entire electron transport chain and when combined with estimations of the wavelength-dependent antenna size of PSII (σ_λ) the *absolute* rate of electron transfer originating from PSII can be determined (ETR_{II}). However, these measurements require advanced, expensive instrumentation and calibration procedures, making them unsuitable for feedback mechanisms between real-time photosynthesis and cultivators (PBR's). In chapter four of this thesis, a method is proposed to probe photosynthesis in a rapid and non-invasive manner using the two devices developed in previous chapters. This previously undocumented method uses the polyphasic rise of chlorophyll *a* fluorescence to determine the *absolute* maximum rate of photosynthetic electron transport. As the method uses rapid inductions (1 second measurements), continuous measurements were employed to track electron transport across a daily growth cycle in the green microalga *C. vulgaris* at a previously undocumented time-series resolution. Additionally, using the information gathered, the method is applied to the Phenobottles to modulate the rate of photosynthetic electron transport which results in altered growth rates. This demonstrates the ability of the developed devices to apply novel measurements to modulating the growth of microalgae in cultivators.

In the final chapter of this thesis an overview of how the research objectives of this work has been answered through the experiments and instruments presented. From here a perspective on where microalgal research could be heading is proposed. The

future applications of the presented devices are explored and the overall significance of this work is discussed.

2. A GUIDE TO OPEN-JIP, A LOW-COST OPEN-SOURCE CHLOROPHYLL FLUOROMETER

A chlorophyll *a* fluorometer was designed and constructed as a tool for assessing photosynthetic phenotypic traits in microalgae and terrestrial plants. This includes 3D modelling the scaffold, 3D printing the device, designing electronic circuits and printed circuit board (PCB) and custom programs. The device is compared to commercial instrumentation to assess its ability to accurately resolve the polyphasic rise of chlorophyll *a* fluorescence. A number of species of both microalgae and plants were assessed to demonstrate the versatility of the instrument. This chapter is a reformatted and upgraded version of a published manuscript in Photosynthesis Research [57].

2.1 Introduction

Chlorophyll *a* is the primary photosynthetic pigment found in all photosynthetic organisms [37]. In phototrophic organisms, part of the energy that is absorbed by chlorophyll *a* molecules is converted into biochemical energy and used to drive photosynthesis (photochemistry). However, a portion of the absorbed energy is either dissipated as heat (non-photochemical quenching) or re-emitted as chlorophyll *a* fluorescence. Through the assessment of chlorophyll *a* fluorescence, inferences can be made regarding the functioning of photosynthetic pathways [59]. These inferences provide a non-direct estimate of the health of the phototrophic organism [77].

The foundation of chlorophyll *a* fluorescence and its interpretation is based on the work of [58]. They proposed that the intensity of chlorophyll *a* fluorescence corresponds to the redox state of the functional photosynthetic units (referring in

particular to the reaction centre of Photosystem II, also known as PSII or RCII). For example, when all PSII reaction centres are oxidized (such as when the plant is in the dark), the fluorescence yield would be at a minimum. However, once exposed to light, PSII reaction centres would become reduced resulting in higher chlorophyll *a* fluorescence emission. Based on this phenomenon, plant scientists have proposed several parameters to quantify the plants photo-physiological state. The most widely used parameter being the maximum quantum yield for primary photochemistry, also known as F_v/F_m [78].

Three main fluorometric approaches exist for the assessment of chlorophyll *a* fluorescence: (1) Pulse Amplitude Modulated (PAM), (2) Fast Repetition Rate (FRR) and (3) Fast rise of the chlorophyll *a* fluorescence or OJIP fluorometry. Each method integrates different aspects (temporal, spectral and spatial) of the chlorophyll *a* fluorescence signature. The focus of this work will be on OJIP (acronym based on the presence of three main phases O-J, J-I and I-P) fluorometry. OJIP fluorometry uses an excitation light source to drive photosynthesis which concurrently triggers chlorophyll *a* fluorescence emission. The O-J (photochemical) phase is well characterised and corresponds to a reduction of PSII's primary acceptor (Q_A). The thermal phases (J-I and I-P) are still debated amongst researchers, but generally the J-I phase corresponds to a reduction of the plastoquinone pool (PQ-pool) and I-P refers to a saturation of electrons on the acceptor side of photosystem I (PSI) [64]. When plants are stressed such as the result of high temperatures, a rapid change in phase can appear in OJIP transients, this is known as a K-step, corresponding to degradation of the oxygen-evolving-complex (OEC) [79]. In order to reduce all PSII reaction centres, the sample must be illuminated with a saturating irradiance higher than 1,800 μmol of photons m^{-2} s^{-1} [59, 80]. The result of this measurement is the rapid polyphasic rise of chlorophyll *a* fluorescence. To analyse this complex feature, an assessment known as the *JIP-test* was developed for easy quantification of OJIP transients [81].

Typically, an OJIP fluorometer is composed of a PIN photodiode as a detector and an LED (or LED array) as an excitation source [62]. The photodiode is pro-

tected by a band pass (680 nm) or long pass (>680 nm) filter which allows only chlorophyll *a* fluorescence to pass. Incoming photons from the filtered chlorophyll *a* fluorescence is detected by the photodiode and creates a voltage potential, which is then measured by a 10-bit data acquisition device (DAQ). The technical challenges of these instruments are that: 1) the detector and DAQ must be be fast enough to detect the fluorescence intensity during the first 100 μs of illumination to be able to assess the value of the fluorescence value when all PSII are oxidized and open (F_o); 2) The photodiode must be sensitive enough to detect the chlorophyll *a* fluorescence which is only 1-2% of total absorbed light [59]; 3) Light intensity from the excitation LED must remain constant throughout the one second measurement to ensure no decrease in fluorescence intensity.

There is a diversity of chlorophyll *a* fluorometers on the market; however, the minimum cost of a commercial device is at least US $1,000. When multiple units are required, such as with high-throughput phenotyping, this becomes an expensive option. In addition, most commercial instruments allow a limited degree of customisation both from a hardware and software perspective, which limits the researches experimental design. For this reason, we present a fully customisable chlorophyll *a* fluorometer for OJIP and quantum yield assessment, for which construction costs less than US $100. To keep the costs down, we have integrated 3D printing and low-cost off-the-shelf electronics to develop a simple open-source OJIP fluorometer (known as Open-JIP), which can be assembled and used without prior coding or electronics experience. The device comes in two forms, Open-JIP (Algae) for microalgal cells in suspension and Open-JIP (Plant) for terrestrial plants.

2.2 Materials and Methods

2.2.1 Setup and Construction

Both designs of Open-JIP (Algae/Plant) were modelled in Fusion360 (AutoDesk, California, USA) and 3D printed in black PLA plastic (inkStation, Sydney, AUS; Figure 2.1; models are available to download at https://github.com/HarveyBates/Open-

JIP. Open-JIP (Plant) was designed around a quick-action clamp (Quick-Grip Medium Bar Clamp, Irwin, Box Hill, Victoria) for which the 3D printed models can be mounted, allowing the user to measure OJIP transients without removing or damaging leaves.

An Arduino microcontroller (Arduino, Mega 2560 Rev3, Somerville, USA) was used to control both Open-JIP configurations (Algae and Plant) (Figure 2.1). This microcontroller was chosen because of its 256-kbit memory which is needed to capture the fluorescence signal along with corresponding timestamps. The microcontroller has a worldwide distribution which makes it easily accessible for anyone interested in photosynthesis.

To detect chlorophyll *a* fluorescence, an operational amplifier (LM358, Texas Instruments, Dallas, USA) was chosen due to its ability to use a single power supply (+12V) and its low power consumption. To adjust the sensitivity of the device, the resistor value (R1) can be switched to a higher resistance for more sensitivity (very dilute cultures) or lower resistance for less sensitivity (concentrated cultures) (Figure 2.2). While a variable resistor could be implemented here (at resistor value R1), the parallel requirement of changing the capacitor (C1) to prevent overshooting of the operational amplifier would negate its customisability. Future versions of the Open-JIP circuit may provide additional gain settings. Additionally, the gain can be adjusted through the software of Open-JIP. Specifically, this can be performed by changing the Arduino internal reference voltage to either 1.1 V, 2.56 V or the default 5 V with a simple one-line command in the Arduino integrated development environment (IDE).

Open-JIP's excitation LED circuit is powered by a 15 V 1.2 A barrel plug switching power supply (15DYS618, Ideal Power, Texas, USA) (Figure 2.2). This circuit provides a saturating irradiance to the microalgal culture (or plant leaf) to induce chlorophyll *a* fluorescence. To obtain constant brightness of the excitation LED, the 15 V coming from the power supply passes through a 12 V linear voltage regulator (KA7812ETU, On Semiconductor, Arizona, USA). Although the switching power supply could provide power to both the LED and photodiode circuits, the sensitivity

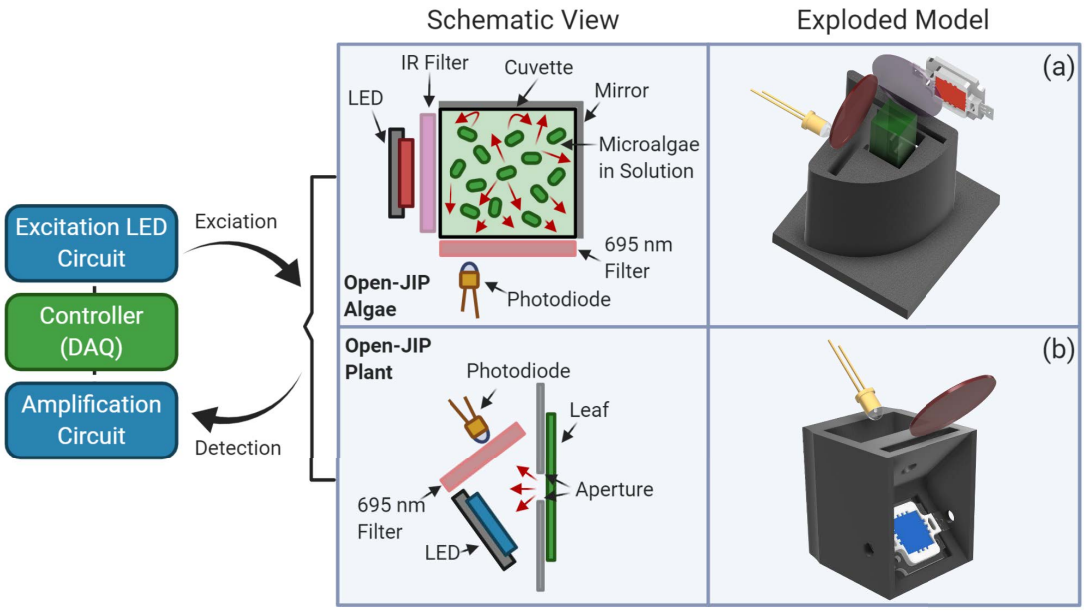

Fig. 2.1: **Block diagram of the Open-JIP instrument**. The microcontroller sends an electrical signal to excitation LED circuit resulting in chlorophyll excitation. The photodiode circuit detects and amplifies the fluorescence signal and sends this information as a voltage to the DAQ (microcontroller) which converts it into usable information via an analog-to-digital converter (ADC). In the schematic view red arrows demonstrate fluorescence excitation. Both (a) Open-JIP (Algae) and (b) Open-JIP (Plant) are shown; however, excitation for the two devices is operated separately.

of the latter requires a highly stable DC supply. This resulted in the use of a 3.7 V 2.4 Ah lithium-ion polymer (LiPo) battery to power the sensitive components (photodiode circuit) of the fluorometer (Figure 2.2a). The voltage of the battery was boosted using a DC-DC boost converter to roughly 18 V (DFR0123, DFRobot, Shanghai, ROC) and then regulated to 12 V using a linear regulator (L7812CV, Jameco, California, USA). This serves two purposes; 1) being that a higher voltage applied to the photodiode circuit (the operational amplifier in particular) provides increased resolution of the chlorophyll *a* fluorescence and 2) as the battery loses charge, the gain of the operational amplifier will remain stable at 12 V.

When a fluorescence measurement is initiated by the user, the microcontroller (Arduino Mega) sends a signal to activate a transistor (T1); resulting in the LED switching on. The switching on (rise time) of the LED must be faster than 50 μs

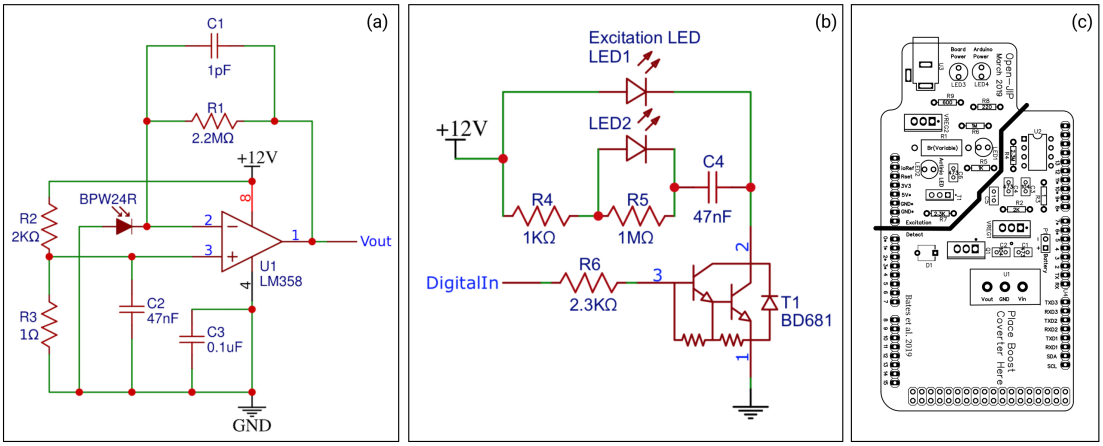

Fig. 2.2: **Schematic of the detection and excitation circuit, and PCB diagram of the Open-JIP fluorometer**. Schematic (a) demonstrates the detector componentry surrounding a LM358 operational amplifier (U1) which is used to amplify the fluorescence signal. Schematic (b) shows the componentry used to switch (T1) on the excitation LED (LED1). The excitation LED (LED1) switches on and off the actinic light when the user wants to measure an OJIP curve. Printed circuit board (PCB) design (c) allows the user to use the fluorometer without modification.

to ensure that a F_o value (minimum fluorescence intensity) can be obtained which is not a result of low actinic light (<1,800 μmol photons m^{-2} s^{-1}). To achieve this the Darlington Transistor (BD681, Farnell, Leeds, UK) (T1) in conjunction with a parallel diode and resistor arrangement was used; resulting in a rise time of 40 μs. The parallel arrangement also prevents a bright flash from the excitation LED when switching on and gives a steady excitation intensity for the entire one second measurement. For up-to-date versions of the Open-JIP circuitry see our GitHub page (https://github.com/HarveyBates/Open-JIP).

2.2.2 *Benchmark Tests*

To demonstrate the devices accuracy, reproducibility and sensitivity a number of tests were conducted comparing Open-JIP's measurements to a commercial chlorophyll *a* fluorometer (FL3500, PSI, Drasov, Czech Republic). These experiments and benchmark tests are demonstrated in subsequent sections.

2.2.3 Biological Material

Microalgae of two different taxa were chosen, (1) *Chlorella vulgaris* (UTS-LD) (Phylum Chlorophyta) and (2) the marine microalga *Synechococcus sp.* (CS-29) (Phylum Cyanobacteria). *C. vulgaris* was grown in MLA medium at 20 μmol photons m^{-2} s^{-1} under white LED globes, measured with a 2π light meter (LI-250A, LiCor, Nebraska, USA) [82]. *Synechococcus sp.* was grown under the same lighting conditions with different media (Pro99 Media) [83]. Three different species of higher plants were chosen (a) *Spathiphyllum wallisii*, (b) *Citrus hystrix* and (c) *Spinacia oleracea* as they present vastly different OJIP transients and demonstrate Open-JIP's ability to quantify different phenotypes.

2.2.4 Experimental Design

Aliquots (4 mL) were taken from a stock culture of *C. vulgaris* during its exponential phase and transferred into 10 x 10 mm disposable fluorescence cuvettes. Samples were placed in both the commercial instrument (FL3500) and in Open-JIP (Algae) both of which were calibrated to an actinic light intensity of 2,100 μmol photons m^{-2} s^{-1}. These samples were given five minutes to dark-adapt (obtain a reproducible reference state) before simultaneously measuring OJIP curves for one second in each of the two devices. After which the cuvettes were gently shaken to ensure the algae remained suspended in solution and another five minutes were given to allow the algae to dark adapt before repeating the experiment two more times. The experiment was then repeated with *Synechococcus sp.*

As a complementary test, changes in chlorophyll *a* fluorescence induction were measured using a heat treatment with a *C. vulgaris* culture, as demonstrated previously by [84] with the higher plant *Arabidopsis*. Six aliquots of *C. vulgaris* were placed inside an oven at 60 °C for twelve minutes. OJIP kinetics were then measured with the same technique as described above using both instruments (n=3).

Changes in the O-J kinetics were induced by illuminating *C. vulgaris* cells with different amounts of saturating light leaving five minutes for dark-adaptation be-

tween each of four light intensities. In order to do this, neutral density filters were added in front of the excitation LED of the Open-JIP (Algae) setup, allowing for four different actinic light (at 626 nm) irradiances (14,000, 8,500, 6,000 and 3,200 μmol photons m^{-2} s^{-1}) as measured by a 4π light meter (LI-250A, LiCor, Nebraska, USA).

Open-JIP (Plant) was used to obtain OJIP transients on three species of plants, *S. wallisii*, *C. hystrix* and *S. oleracea*. Each plant was obtained from a local stock and therefore the resulting measurements are purely to demonstrate Open-JIP's ability to resolve the chlorophyll fluorescent transient. A five-minute interval was left between the three replications to allow the samples to dark-adapt. Unlike the tests done on microalgae, this experiment used a blue (466 nm) excitation LED to show the devices ability to use multiple wavelengths to assess OJIP.

2.2.5 Data Analysis

Recorded OJIP curves are copied from the serial monitor of the Arduino software (Arduino IDE, Somerville, USA) and formatted into a .CSV file in excel. Relative variable florescence (V_t) was calculated as:

$$V_t = \frac{F_t - F_o}{F_m - F_o} \tag{2.1}$$

allowing the two devices OJIP kinetics to be compared; as they have different scales for measuring chlorophyll a fluorescence. Data was then plotted using Python (see here for example scripts - https://github.com/HarveyBates/Open-JIP).

2.3 Results

A comparison of the OJIP curves of *Synechococcus sp.* and *C. vulgaris* obtained by Open-JIP and a commercial instrument (FL3500 chlorophyll fluorometer) demonstrates the devices ability to produce accurate and reproducible analysis of the OJIP transient (Figure 2.3). As shown in Figure 2.3, the transients measured by the com-

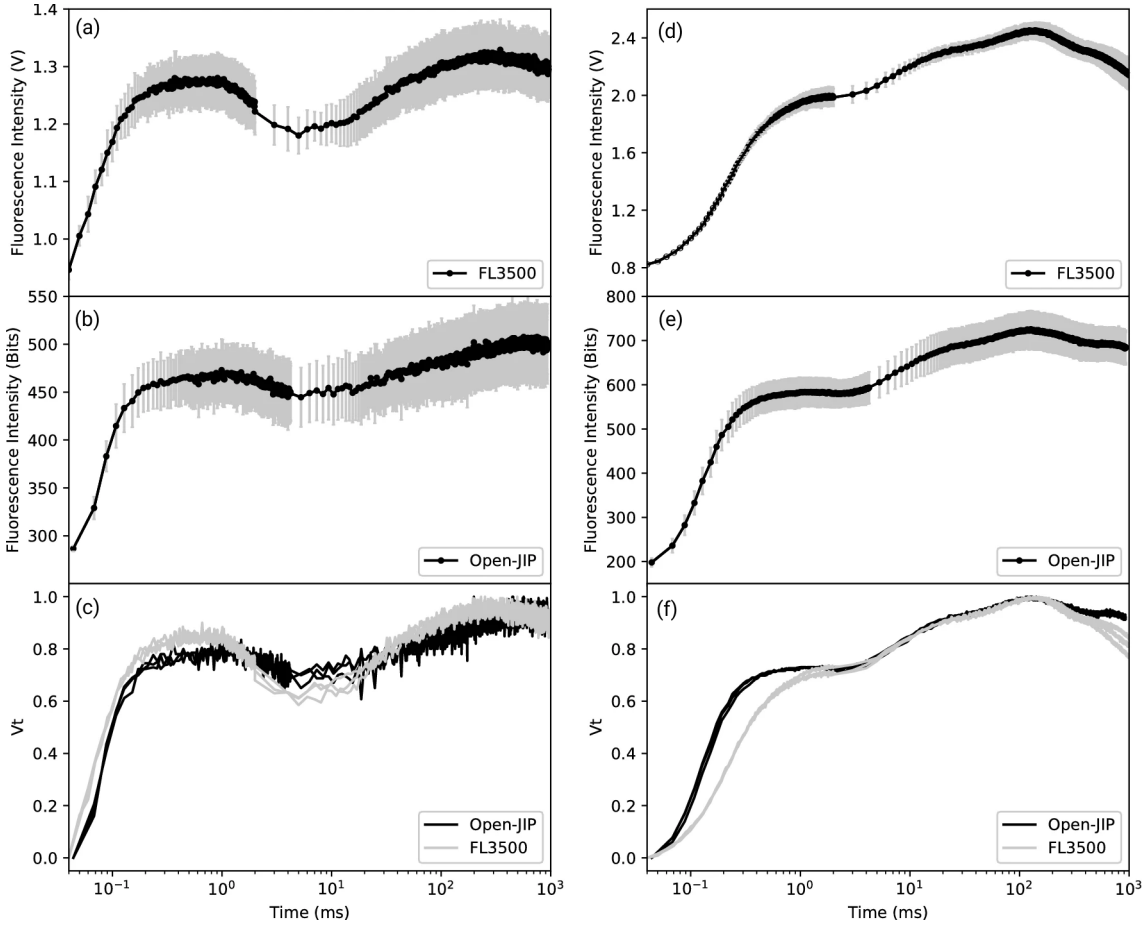

Fig. 2.3: **OJIP transient for *Synechococcus sp.* (CS-29) (a, b, c) and *C. vulgaris* (d, e, f).** Panel c and f demonstrate relative variable fluorescence (V_t) for each of the two microalgae and instruments. Data are averages (n=3) ± SD for panel a, b, d and e.

mercial (FL3500) and the Open-JIP (Algae) were comparable for all samples. Slight variations can be noted in the O-J rise of Figure 2.3f which is the result of different actinic light intensities between the two instruments [85]. Due to differences in the design between the commercial and custom-made instruments, the emitted actinic irradiance will never be identical.

To test the time response of Open-JIP, the effect of light intensity on the rise of O-J phase in *C. vulgaris* was measured (Figure 2.4). As the actinic light intensity of the fluorometer increases, so too does the rate at which fluorescence rises for the O-J phase. The fact that we observed these changes on the O-J phase indicates that Open-JIP has sufficient time resolution to measure the fast components of the chlorophyll fluorescent transients.

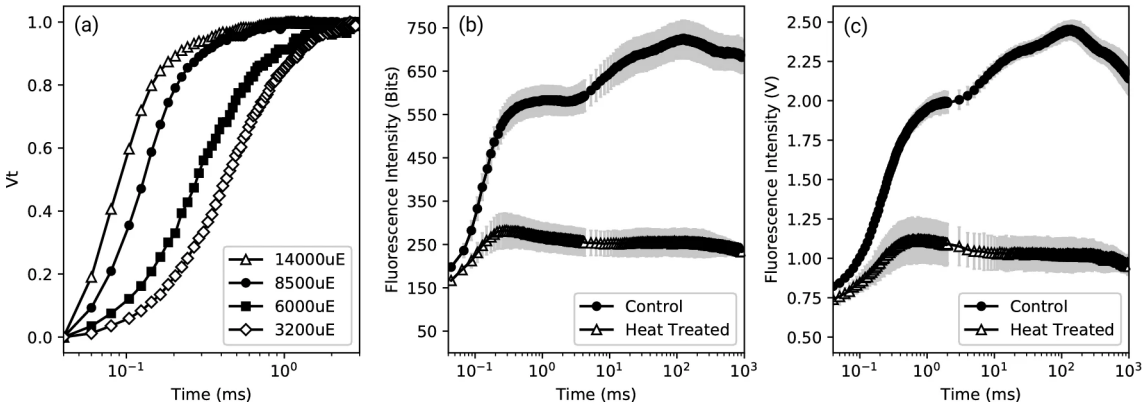

Fig. 2.4: **Effect of different light intensities and heat stress comparison.** (a) On the O-J rise of chlorophyll *a* fluorescence in *C. vulgaris* as measured by Open-JIP (Algae). Relative florescence intensity (V_t) is shown and normalised to 3 ms to better demonstrate this feature. (b) Non-heat treated (black circles) and after twelve minutes at 60°C (white triangles) of the OJIP measured with Open-JIP (Algae) with *C. vulgaris* (n=3 ± SD). (c) Same experiment as in (b) however OJIP transients are measured with the FL3500 fluorometer (n=3 ± SD).

To provide evidence that Open-JIP can be used to assess different phenotypes in photosynthetic organisms, a high temperature stress treatment was implemented. *C. vulgaris* was exposed to a dark incubator at 60 °C for twelve minutes as shown in Figure 2.4bc. Control *C. vulgaris* cells exhibited a three phasic OJIP curve using both instruments (commercial and Open-JIP). As expected, the heat-treated sample showed alterations in the OJIP kinetic for both instruments. The formation of the so-called K-step around 300 μs (a rise in chlorophyll fluorescence occurring at around 300 μs) was detected accurately in both instruments, with the K-step being associated as a clear photosynthetic phenotype in the event of high temperatures [66].

Different species of common vascular higher plants were chosen to demonstrate Open-JIP (Plant)'s ability to resolve various OJIP transients (Figure 2.5). As can be seen, each plant displays vastly different polyphasic rises, each of which can be measured accurately using Open-JIP. The Open-JIP system is capable of quantifying variations in photosynthesis using only a 10-bit system and simple optics.

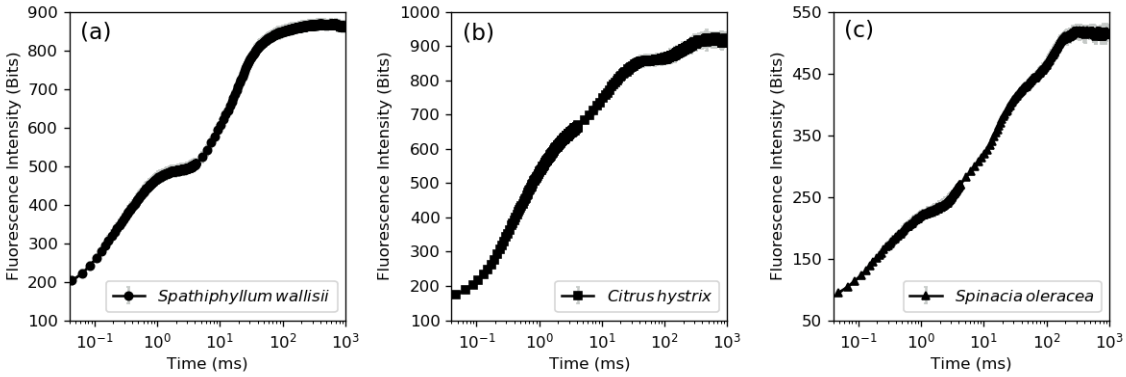

Fig. 2.5: **Open-JIP (Plant) OJIP transients of different species of plants.** (a) *Spathiphyllum wallisii* (black circles), (b) *Citrus hystrix* (black squares), (c) *Spinacia oleracea* (black triangles). OJIP transient measured with Open-JIP (Plant) using a 466 nm actinic light. Data are averages (n=3) ± SD.

2.4 Discussion

In the present work, we have shown the feasibility of building an OJIP fluorometer for less than US $100. Open-JIP has demonstrated accuracy and time resolution that is comparable to commercial chlorophyll *a* fluorometers. A commercial open-source microcontroller (Arduino Mega) is suitable for this work and acts as a microcontroller, DAQ and PC interface. Also, we have shown that even at 10 bits of digitisation (1,024 values), we can still resolve the main features of the OJIP curve and accurately estimate F_v/F_m. It is important to note that other Arduino boards such as UNO, Micro or Nano are not suitable for this task due to limitations internal memory.

The Open-JIP fluorometer has many advantages when compared to commercial instrumentation. The instruments low-cost, allows for its mass production and can be used in high throughput experimental designs. In addition, the ability to fully customise the devices software and hardware (due to it being open-source), allows users to adapt it to their own experimental designs (see https://github.com/HarveyBates for example modifications). Finally, the simplicity of the device allows users with no electronics and/or programming knowledge to construct and use the instrument.

While the aforementioned advantages would make it attractive for some researchers, one has to bear in mind that the Open-JIP is not intended to substitute the use of commercial instruments. Cable widths/lengths and electronic brands would play an important role in the intrinsic variability between instruments, as such changes would alter electronic noise and performance. Therefore, one needs to have at least one commercial instrument to cross calibrate the Open-JIP and to verify its accuracy. Another limitation is that Open-JIP has a reduced digitisation depth (10 bits, 1,024 values) in contrast to commercial instruments, which have depths of 12 to 16 bits (4,096 – 65,536 values), meaning that the resolution of the Open-JIP fluorometer is inferior to expensive OJIP fluorometers; however, this is not a serious limitation considering the devices low-cost.

While in some laboratories it is common to build-in-house instruments; fully open-source fluorometers are far less common. For example, [86] have shown that it is feasible to build a low-cost multicolour FRR fluorimeter for less than US $700. The higher cost of that instrument when compared to Open-JIP is due to its higher complexity as it uses a more sophisticated DAQ and optics. Another earlier example is the work of [87] whom developed a phytoplankton fluorescence device with an estimated cost of US $150; however, the intention of this instrument was not to study photochemical reactions rather growth. The development of Open-JIP provides a low-cost analytical tool for biologists, that is customisable. This is the main benefit of the instrument, as novel biophysical applications require novel and modifiable instrumentation to suit the researchers' requirements. In particular, the customisability of the device would allow scientists in the future to add, modify and explore other protocols that will aid understanding the complexities of the OJIP polyphasic rise. Examples of these modifications could include different wavelengths, sampling rates, optical configurations and data acquisition devices (see https://github.com/HarveyBates/Open-JIP for more information).

Open-JIP is to be used as a low-cost sensor for high-throughput measurements, for example in algal phenomics whereby the user requires several fluorometers to measure phenotypes simultaneously [25]. Open-JIP is an example of open-source

scientific instrumentation that will enhance the outreach of the OJIP method to a wider group of users in developing countries, citizen scientists and students.

3. PHENOBOTTLE: AN OPEN-SOURCE PHOTOBIOREACTOR FOR NOVEL PHYSIOLOGICAL STUDIES

A photobioreactor was created to assess real-time photosynthetic and growth phenotypes in real-time. This device is another low-cost instrument that is focused on assessing photophysiology in microalgae in a reproducible manner. However, the device also has the ability to culture the microalga while probing photosynthesis. This results in a time-series assessment of photophysiology which is unrivalled by similar instrumentation. This is a reformatted version of a manuscript which is under review by Algal Research.

3.1 Introduction

Microalgae are unicellular photosynthesising organisms that contain chlorophyll *a* as their primary light harvesting pigment [1, 88]. As a result of their high biodiversity, microalgae are able to inhabit a wide range of environments [1, 3, 4]. Their rapid growth rates and biochemical/metabolic diversity has placed microalgae at the forefront of biotechnological research into renewable energies, climate change mitigation and pharmaceutical research [89–93]. Such research provides invaluable information on the optimisation of microalgal production for commercial operations [32, 94].

As microalgae live in dynamic environments, they exhibit a large degree of phenotypic plasticity in their photosynthetic functions [95, 96]. Mapping these photosynthetic properties (or traits) under an array of environmental conditions can be done using a photobioreactor (PBR). PBR's can create a reproducible reference state for which to compare the physiological condition of microalgae as a response to changes in environmental variables [97, 98]. However, to ensure that microalgae are in a

stable reference state, automated measurements must be taken at a high temporal resolution whilst also using accurate instrumentation. High temporal resolution is particularly important, as photosynthesising organisms possess the ability to rapidly regulate light harvesting within seconds in response to changing environmental conditions so as to avoid over-excitation [99]. Rapid changes in photosynthesis therefore need to be probed in near-real time to identify the mechanisms that fine tune the photosynthesis of microalgae.

Some commercial PBR's have been developed to replicate real-world environmental conditions (i.e. fluctuating light to simulate cloud cover) [100], whilst others are manufactured for specialised experimental designs under controlled laboratory conditions [101]. Additionally, there are custom-built microfluidic PBR arrays available for high throughput screening of microalgae [31]. The microfluidic system designed by [31], provided an extremely high-throughput (250 times higher throughput that traditional culturing methods) technique for assessing lipid content in microalgae. However, the low volume used in their microfluidic system did not scale growth rate when compared to larger volume experiments.

As most commercial PBR's have a limited degree of user customisability, researchers are driven to choose experimental methods within the technical constrains of the available equipment. An alternative approach would be a completely customisable instrument, whereby both software and hardware can be customised to provide researchers with the ability to develop their optimal experimental designs. Measuring frequency and accuracy should be high to capture real-time physiological processes and the cost of the instrument should be low to allow for an array of PBR's to screen environmental conditions, simultaneously. Furthermore, these devices must have a large enough volume to allow for aliquots to be extracted for external analysis such as chemical and biochemical assays, metabolomics, or genomics of the microalgal culture.

For these reasons, in this work, we present the Phenobottle, a PBR designed for customised physiological studies whereby researchers define specific hardware and/or experimental procedures. This device is comprised of 3D printed compo-

nents, off-the-shelf electronics, and common laboratory-based plastic ware to create a cost-effective device. The user is provided with all the instructions to construct, code, and use the Phenobottle without the need for prior coding or electronics experience. The current version provides control over irradiance, mixing through a vertical magnetic stirrer, bubbling of ambient air or CO_2 (with use of external CO_2 supply) and assessment of the physiological state of microalgae through several integrated sensors. These sensors include optical density, temperature and a modified open-source OJIP chlorophyll a fluorometer [57]. Each sensor can monitor physiological traits from a dilute to concentrated culture and can be adjusted in a multitude of ways (software and hardware adjustments) to accommodate for different species of microalgae. The chlorophyll *a* fluorometer provides a basic assessment of photosynthetic phenotypes through variable fluorescence (F_v) and quantum yield of photosystem II (F_v/F_m). In addition to this, the entire kinetic of the polyphasic rise of OJIP chlorophyll *a* fluorescence can be derived for advanced analysis of the light reactions of photosynthesis (for a more detailed introduction to OJIP fluorescence see [64, 81]). In addition to this, data collected from the integrated fluorometer can be used to find correlations with more labour intensive techniques that explore alternative phenotypes (as in Chapter 4 of this thesis). The Phenobottles basic operations are demonstrated through a benchmark test using the green-alga *Chlorella vulgaris*.

3.2 Materials and Methods

3.2.1 Phenobottle Hardware Design

The structure of the Phenobottle is based around a 75 cm^2 cell culture flask (Falcon Flask, Corning, NY, USA). The Phenobottles structure was 3D modelled in Fusion360 (AutoDesk, California, USA) and 3D printed using black PLA plastic (inkStation, Sydney, Australia) (Figure 3.1). For more information about version releases please visit: [102].

Two types of digital control units were used to operate electronic components in the Phenobottle, a Teensy 3.6 (PJRC, Oregon, USA) and a Raspberry Pi (RPi) (3B+, Cambridge, UK). The RPi is used as the control over all operations of the Phenobottle (master). On top of each RPi a Motor HAT (Adafruit, NY, USA) provides individually controlled pulse width modulated (PWM) power to motors, lights and pumps. This configuration allows the user to control the speed of the motors and irradiance of the lights within the software of the Phenobottle. The system was powered by a 12 V 2 A power supply (15DYS624, Ideal Power, Texas, USA). Light was provided by LED strips positioned on the back wall of the Phenobottles main frame. RGB LED's (RGB LED Bare, Core-Electronics, Kotara, Australia) were used to allow the modification the light spectrum to match the photosynthetic antenna requirements of different algae. This is required for experiments examining the optimisation of growth, as different species possess different light harvesting complexes [103, 104].

A reversed vacuum pump (Vacuum Pump 12 V, Core-Electronics, Kotara, Australia) bubbled air or CO_2 (with external CO_2 supply) into the culture flask. Mixing of the microalgae is accomplished via a magnetic stirring rod (756, Labdirect, Sydney, Australia) inside the culture flask. The rod is spun by a 12 V DC motor (YM2716, Jaycar, Rydalmere, Australia) which has a 3D printed magnetic holder on the shaft. The magnetic holder houses two neodymium disc magnets (20079B, AMF Magnets, Texas, USA) which are connected such that the magnetic rod inside the flask is pulled against the wall of the flask and follows the spin of the mixing motor. A 3D printed bottle cap was designed to allow for five separate tubes to access the culture. These tubes provide the microalgae with air and give the user access to the microalgal culture through a needless intravenous (IV) connector (BD Q-SyteTM, BD, New Jersey, USA). The other tubes are connected to a laboratory-created flow through cell connected to a peristaltic pump for chlorophyll *a* fluorescence analysis.

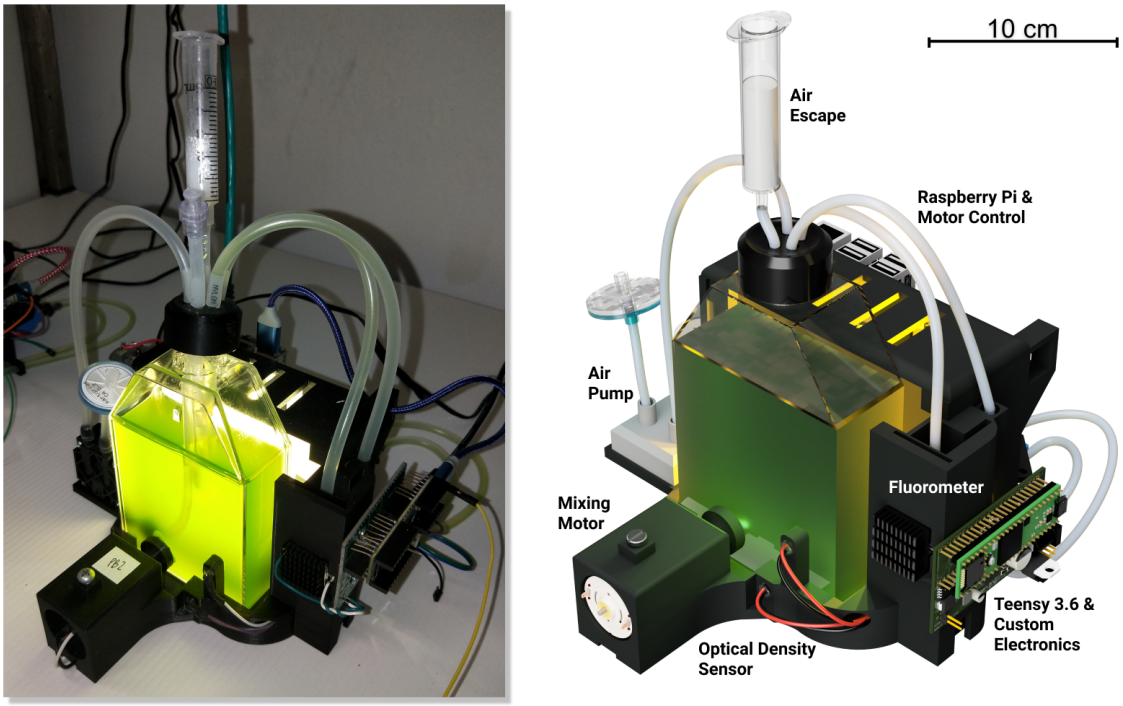

Fig. 3.1: **Photograph (Left) and 3D render of a Phenobottle (Right).** The 3D printed shell of the Phenobottle is designed to fit specific components but can be easily adjusted (via 3D modelling) to accommodate different motors, lights (white illumination displayed here) and/or electronic infrastructure. On the rear of the Phenobottle is a Raspberry Pi computer which is connected via USB to the Teensy 3.6 microcontroller and custom electronics.

3.2.2 Custom Electronics

Having developed and designed the custom electronics a printed circuit board (PCB) was constructed using EasyEDA (Version 6.2.44, Guangdong, China) and manufactured by JLCPCB (Guangdong, China). The circuit board features all the necessary components to measure optical density, temperature and chlorophyll *a* fluorescence (circuit board and schematics available at [102]).

3.2.3 Measurement of Optical Density

Optical density was measured using two identical 875 nm LED's (SIR333-A, Everlight, New Taipei City, Taiwan). These LED's were positioned on opposite sides of the bottles with a path length of 38 mm and secured with clear epoxy resin (Ultra

Clear Araldite, Selleys, NSW, Australia). Light from the emitting LED is directed through a pinhole (2 mm diameter) before passing through the culture and being detected by the detecting LED.

As a detector, we have used the same LED as the emitter in reverse bias (negative terminal connected to positive and positive connected to negative). This configuration results in incoming photons from the emitting 875 nm LED to create a voltage that can be measured by the Teensy 3.6. This voltage is amplified to a usable range for the Teensy 3.6's analog-to-digital converter (ADC) with use of a feedback resistor (2.6 MΩ). As a result of this arrangement the user can adjust the sensitivity of the optical density sensor to suit their culture density by either adjusting the resistor value or by adjusting the reference voltage in the Teensy 3.6 code (between 1.1 and 3.3 V).

To calibrate the OD sensor the user must place a culture flask with growth medium in the Phenobottles designated slot and measure a baseline transmission reading (I_o). This value is added to the scripts on both the Teensy 3.6 and RPi, allowing the Phenobottles to automatically calculate optical density (OD) according to the Beer-Lambert. Doubling time of microalgal cells in solution (k) was calculated according to [105], using of both continuous measurements of optical density and a cross calibration with manual cell counts.

$$OD = -\log_{10} \frac{I}{I_o} \tag{3.1}$$

Where I is the transmitted light through the microalgal solution.

$$k = \frac{\log_2(\frac{N_t}{N_0})}{\Delta t} \tag{3.2}$$

Where k is the doubling time of microalgal cells per unit time (24 hours), N_t is the final cellular concentration after 24 hours and N_0 is the cellular concentration at the start of the doubling period.

3.2.4 Measurement of Temperature

A simple temperature sensor (TMP36, Analog Devices, Massachusetts, USA) was utilised as an external indicator of local air temperature. We employed a temperature-controlled room to maintain temperature continuity between replicate Phenobottles.

3.2.5 Architecture for Chlorophyll a Fluorescence Analysis

Chlorophyll *a* fluorescence was assessed using a modified Open-JIP fluorometer [57]. A peristaltic pump (50220, Makeblock, Shenzhen, China) was used to sub-sample the microalgal culture from the culture flask through a custom-made flow-through cuvette arranged for a 90 degree angle between emitted and detector. The design of the cuvette uses two irrigation adapters (1010024, Pope, Kilkenny, Australia) glued (Aquafix Waterproof Epoxy, Selleys, NSW, Australia) to either end of a polystyrene spectrometer cuvette (C5291, Sigma Aldrich, NSW, Australia). Silicone tubing (5 OD x 3 ID mm) (310-0305, Gecko Optical, Joondalup, Australia) was connected onto either end of the cuvette, allowing the algal cells to be dark-adapted inside the cuvette before measuring their chlorophyll *a* fluorescence signature. The direction of flow from bottom to top of the cuvette eliminates the possibility of air bubbles affecting measurements.

Maximum actinic light intensity from the fluorometer was set to 2,600 μmol photons m^{-2} s^{-1} with a 4π light meter (LI-250A, LiCor, Nebraska, USA) at a peak wavelength of 626 nm. The intensity of the actinic light was adjusted with the use of a 0.9 neutral density (ND) filter (Lee Filters, Hampshire, UK). This can also be achieved by adjusting the electrical configuration of the actinic light circuitry. As different species of microalgae have different antenna complexes, Phenobottles have the option to use four different actinic light sources (466, 532, 592 and 626 nm) in order for the user to select the correct LED excitation for their algal species of interest [57, 106].

3.2.6 Chlorophyll a Fluorescence Analysis

Photophysiological traits were assessed through quenching analysis of chlorophyll a fluorescence (Figure 3.2) [64, 80]. A one second excitation of the sample induces the polyphasic rise of the chlorophyll a (OJIP transient) fluorescence that could be used acts as a surrogate to the redox state of Photosystem II (PSII)[64]. Several derived parameters can be obtained from an OJIP transient using the so-called JIP-test algorithm [81]: F_o (O-step) is the minimum level of fluorescence; F_j (J-step) which represents a reduced primary electron acceptor (Q_A) of PSII; F_i (I-step) is caused by reduced electron acceptors on the acceptor side of photosystem I (PSI); F_m (P-step) occurs when the entire electron transport chain is reduced; the maximum quantum yield of PSII (F_v/F_m); the maximum quantum yield at the J-step ($\phi PSIIQ_A$) [70]); the variable fluorescence at the J-step (V_j) that is an indicator of the portion of reduced PSII's [64, 80, 107]; the initial slope of chlorophyll a fluorescence (M_0) that is an indicator of reduction rate of Q_A by active PSII's [107]; and the linear electron transport performance index (PI_{abs}).

$$V_j = \frac{F_j - F_o}{F_v} \tag{3.3}$$

$$M_0 = 4ms \times \frac{F_{300\mu s} - F_o}{F_v} \tag{3.4}$$

$$PI_{abs} = \frac{1 - \frac{F_o}{F_m}}{\frac{M_0}{V_j}} \times \frac{F_v}{F_o} \times \frac{1 - V_j}{V_j} \tag{3.5}$$

To compare fluorescence parameters with different scales, Z-scores (Z) can be used to normalise the values around their mean.

$$Z = \frac{x_i - \overline{x}}{S} \tag{3.6}$$

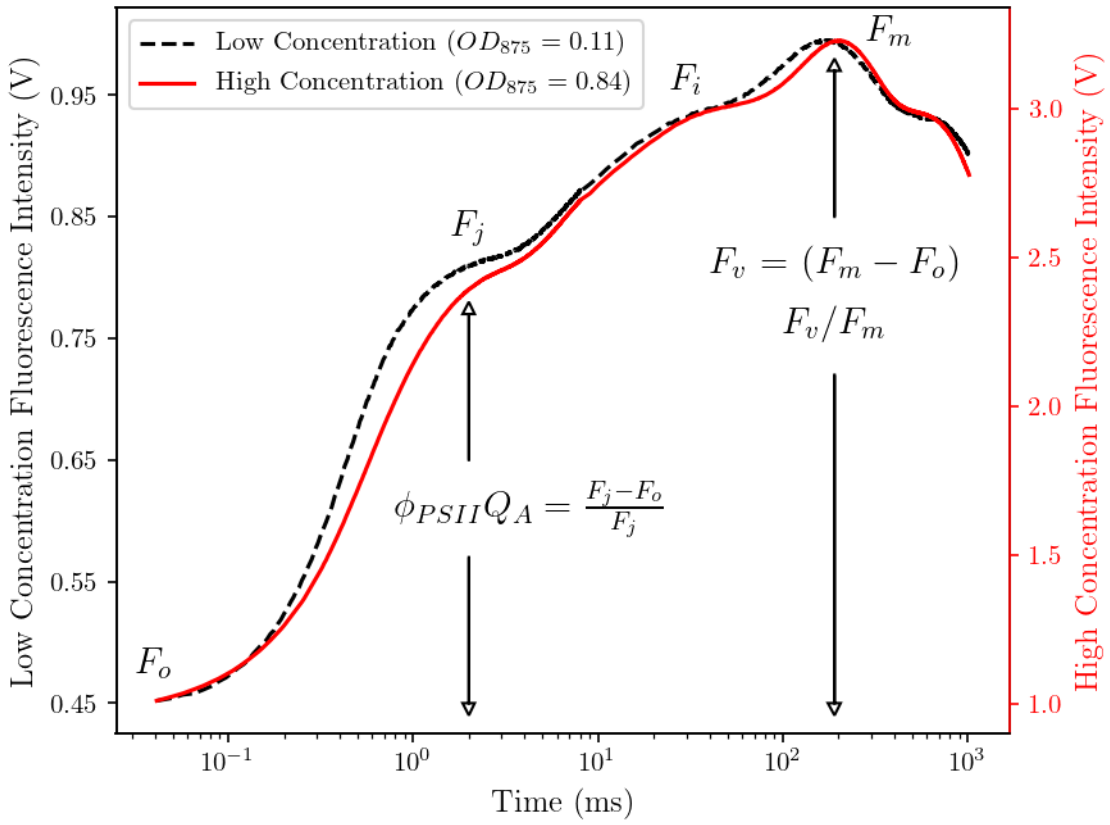

Fig. 3.2: **Visualisation of OJIP chlorophyll *a* fluorescence induction curve and derived parameters.** Two concentrations of *Chlorella vulgaris* are shown to demonstrate Phenobottles ability to assess photosynthesis at both a high (0.84 OD) and low density (0.11 OD). F_o is measured at 40 μs, F_j at 2 ms, F_i at 30 ms and F_m is the maximal fluorescence intensity. Variable fluorescence (F_v) is the difference between F_m and F_o, dividing this value by F_m after dark adapting gives the maximum quantum efficiency of PSII (F_v/F_m). $\phi PSIIQ_A$ represents maximal quantum efficiency of PSII at the J-step.

The average ($\overline{x}$) is subtracted from each value (x_i) and divided by the standard deviation from the mean (S). Z-scores higher than the mean will be positive and those lower will be negative.

3.2.7 Phenobottle Software

Phenobottle hardware is controlled by the RPi through a single Python script (scripts provided at: [102]. The *slave* (Teensy 3.6, coded in C++) reads commands send from the RPi via its USB (serial) port (Figure 3.3). When a request is received by the Teensy 3.6 it proceeds to take the required measurement and sends the data back to the RPi. The data is then decoded, mathematically transformed, and sent to a locally hosted MySQL database running on an additional separate RPi.

To assess photosynthesis and growth while the Phenobottles are operating a plotting graphical interface (PGI) was developed which displays live data. The PGI is programmed with Python and can be used on Windows, Linux and Macintosh operating systems. Additionally, if the user needs remote access while an experiment is running, this can be achieved through virtual network computing (VNC) software (VNC Viewer, RealVNC, Cambridge, UK).

3.2.8 Biological Material

Chlorella vulgaris (Phylum Chlorophyta) (UTS-LD) was chosen for this benchmark test of the Phenobottles. At time of subculturing the culture was in its exponential phase on a 12-12 light dark cycle in MLA media at 65 μmol photons m^{-2} s^{-1} [82].

3.2.9 Benchmark Test

Three separate Phenobottles were used to grow *C. vulgaris* concurrently under controlled conditions to demonstrate the devices ability to produce reproducible and accurate results. MLA media (200 mL) was added to each Phenobottle and a 100% transmission reading of optical density was obtained as described above. Light intensity was set to 65 μmol photons m^{-2} s^{-1}. 30 mL aliquots were taken from a stock solution of *C. vulgaris* and transferred to each of the Phenobottles through the IV-connector. The culture was allowed to stabilise in the bottle for two days on a 16-8 light dark cycle before being diluted to a time zero optical density of 0.05 by extracting cells through the iv-connector and injecting fresh MLA media.

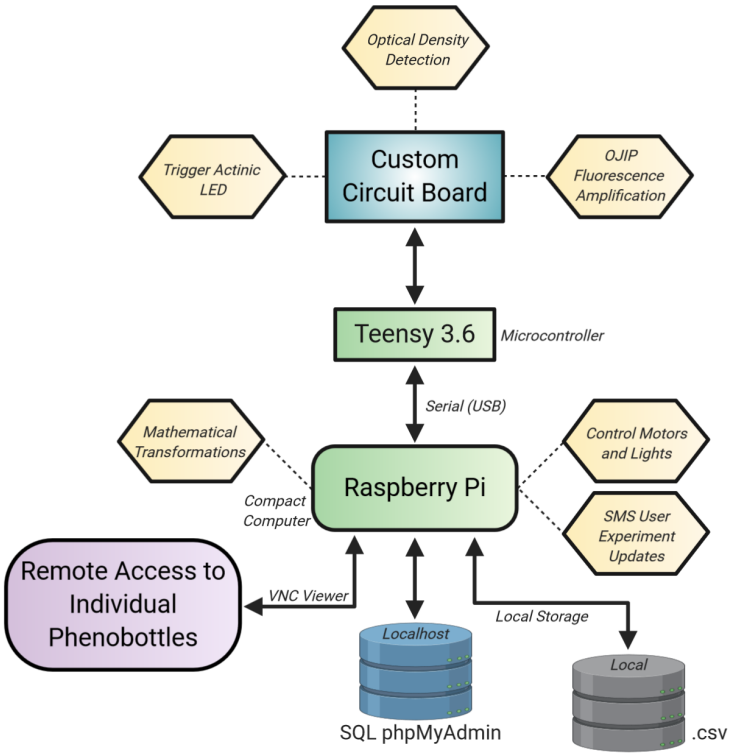

Fig. 3.3: **Operational processes housed within the Phenobottles software and hardware.** The master controller for the Phenobottle is the Raspberry Pi (RPi) (shown with light green background). Requests to the Teensy 3.6 are made from the RPi for measurements to be taken. The RPi has overall control over mixing speed, bubbling intensity, and light intensity. An external RPi locally hosts a Structural Query Language (SQL) phpMyAdmin database for each Phenobottle to connect to and write data into separate dedicated tables. Each Phenobottle also possesses a comma separated value (csv) file of the data if the server cannot be reached. External users can access the data at any time by communicating with the database and plotting the data using Phenobottles plotting graphical interface. To change parameters within the Phenobottle individual Phenobottles can be accessed by a virtual network computing (VNC) service.

The stabilization period helps to ensure the Phenobottles are functioning optimally before starting the experiment. Physiological traits were then monitored with automated chlorophyll *a* fluorescence and optical density measurements taken every ten minutes for a period of 280-hours.

3.2.10 Data Analysis

Function fitting for each plot was preformed using OriginLab (Version 9.7.0.188) and plotted using Python (Version 3.7.4). To explore daily fluctuations in electron transport a heatmap was created using R (Version 3.6.2). Biorender.com was used to create Figure 3.3.

3.3 Results

To assess the accuracy of the optical density (OD) sensor two tests were performed. The first was a calibration between a commercial spectrometer and a Phenobottle using *C. vulgaris* which was fitted to a linear regression ($R^2 = 0.999$) (Figure 3.4A). This comparison was achieved by taking aliquots at different dilutions from a Phenobottle and placing them into a polystyrene spectrometer cuvette to be measured in a UV-Visible spectrophotometer (both measurements were taken at 875 nm). The second calibration involved diluting a Phenobottle containing *C. vulgaris* to various OD's. After which, aliquots were extracted for cell counts which were carried out under a microscope using a Neubauer Hemocytometer chamber. OD values were then plotted against cellular concentration per millilitre (mL) and fitted to a linear regression ($R^2 = 0.988$) (Figure 3.4B).

OD was monitored in three Phenobottles over an experimental period of 11 days from a starting value of ∼0.05 and extrapolated using a logistic function (Figure 3.4c). OD calculations at the beginning of the experiment corresponds to a cell density of 0.1×10^7 per mL and a final value of 2.3×10^7 per mL, corresponding to an increase in *C. vulgaris* cell count per mL of 2,300% in 11 days (Figure 3.4b-c). OD decreased over the dark periods and rapidly dropped upon re-illumination when growth lights were switched back on each morning. Doublings per day decreased following a 2^{nd} order exponential decay ($K_1 = 0.068 \pm 0.079$, $K_2 = 0.009 \pm 0.001$) from 0.982 ± 0.323 after 1 day to 0.098 ± 0.003 after 11 days (Figure 3.4bd).

The maximum quantum efficiency of PSII can be assessed through normalised variable fluorescence (F_v/F_m) (Figure 3.5a). Within 1 hour of the dilution of *C. vul-*

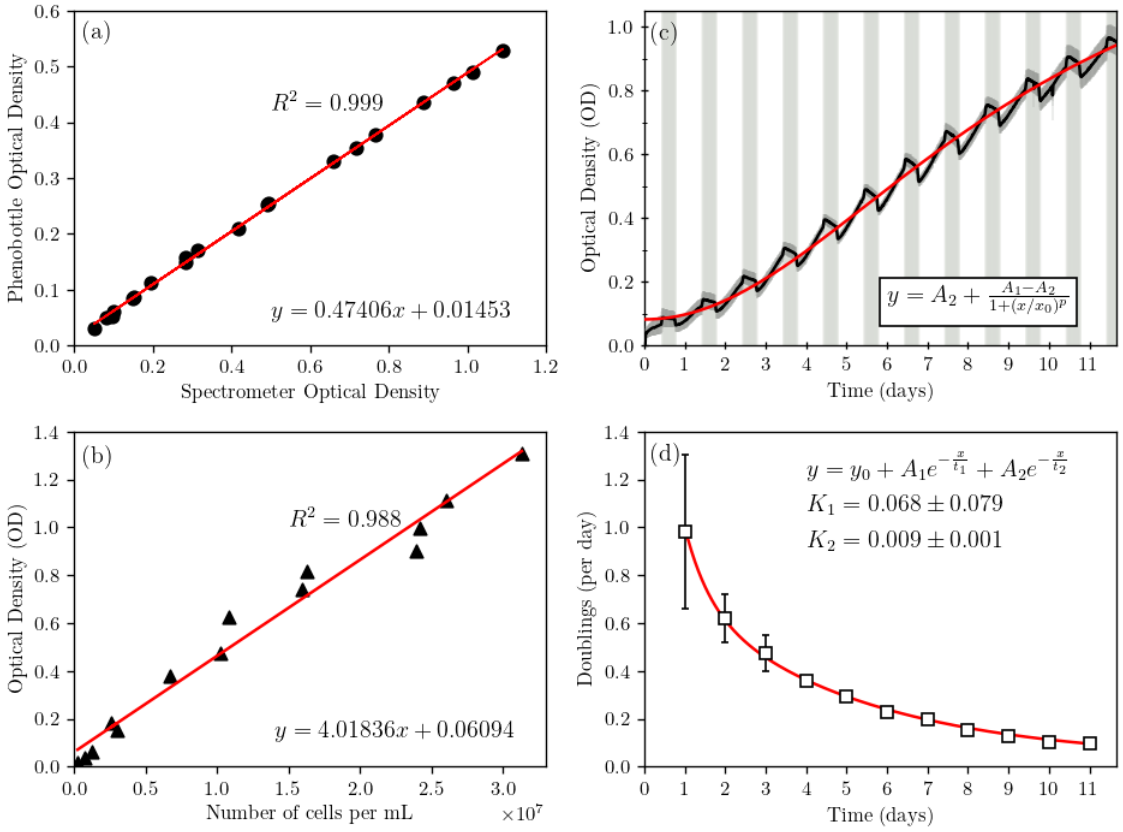

Fig. 3.4: **Optical density calibrations and time-series assessment of growth.** (a) Optical density of *C. vulgaris* measured with the Phenobottle compared to a commercial spectrometer at the same wavelength (875 nm). (b) Optical density as measured by the Phenobottle compared to the number of cells ($\times 10^7$) of *C. vulgaris* per millilitre. Linear regressions were calculated for both A and B. (c) Optical density (black line) measurements taken every 10 minutes over the experimental period (n=3 $\pm$ standard deviation). A logistic (red) line has been extrapolated to the growth curve. Shaded vertical blocks represent times when the growth lights were switched off. (d) Average doubling rate per day of *C. vulgaris* in the Phenobottles (n=3 $\pm$ SD).

garis F_v/F_m was 0.5 $\pm$ 0.04, this was followed by a rapid decline in PSII efficiency to 0.425 $\pm$ 0.02 after 3 hours. For the following 4 days F_v/F_m increases gradually, with periodic declines in quantum efficiency of PSII during dark periods and rapid increases during growth light illumination. These oscillations in F_v/F_m are attenuated after 7 days, with the quantum efficiency of PSII remaining stable at 0.71 $\pm$ 0.02.

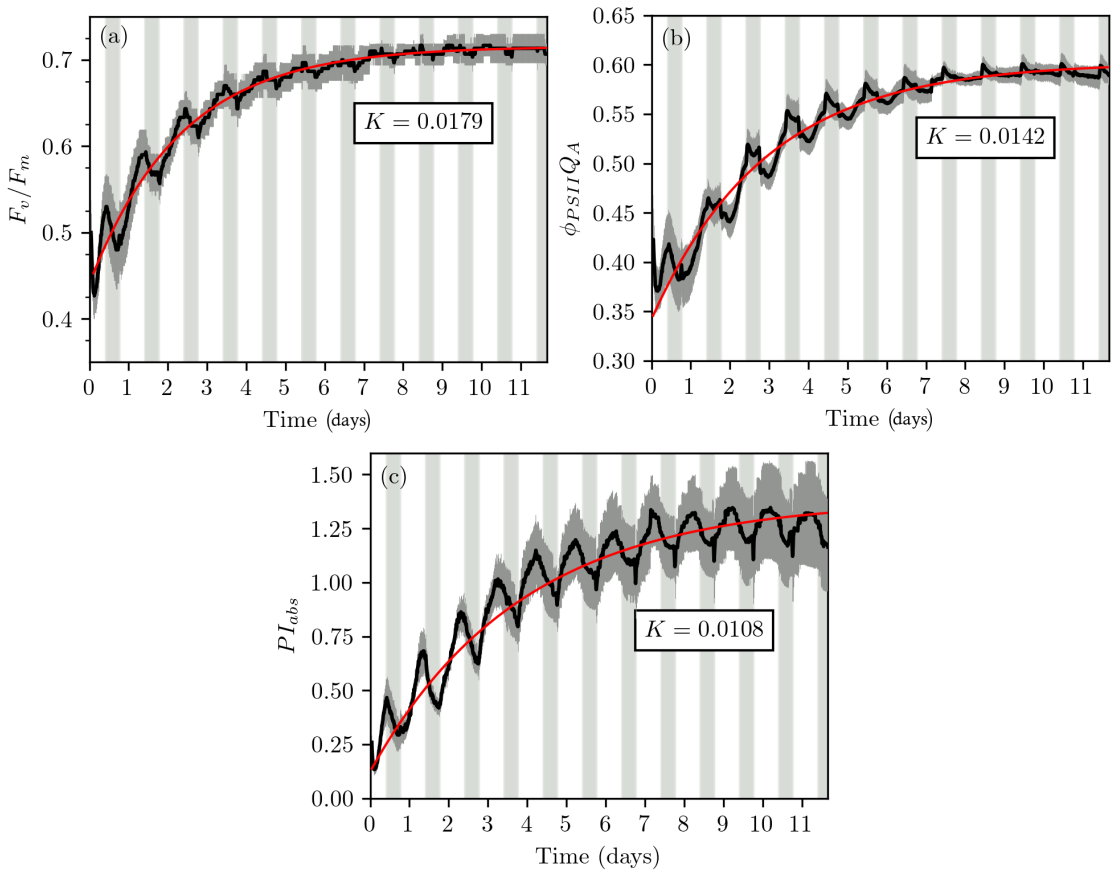

Fig. 3.5: **Time-series assessment of photosynthesis using the Phenobottle** (a) Quantum yield of PSII (F_v/F_m) (b) Maximum photochemical efficiency of PSII at the J-step ($\phi PSIIQ_A$) and (c) Performance index (PI_{abs}) of *Chlorella vulgaris* over a 280-hour period with 16:8 light dark cycles. Measurements were taken every 10-minutes. Dark vertical lines represent times when the growth lights are switched off. Each plot is fitted with an exponential decay (red line) to display a line of best fit ($y = y_0 + A_1 e^{-\frac{x}{t_1}}$) for which rate constants could be calculated(n=3 ± SD).

The maximal quantum efficiency of PSII at the level of Q_A (before re-oxidation of Q_A by downstream acceptors) can be measured through $\phi PSIIQ_A$ (Figure 3.5b) [70]. Quantum efficiency of PSII at the J-step decreases rapidly 1 hour after dilution from 0.42 ± 0.04 to 0.37 ± 0.02 at 3 hours. Similarly to F_v/F_m, $\phi PSIIQ_A$ increases over the first 7 days to a stable value of 0.6 ± 0.15, with gradually attenuated oscillations as a result of diurnal irradiance cycles visible over the 11 day experimental period.

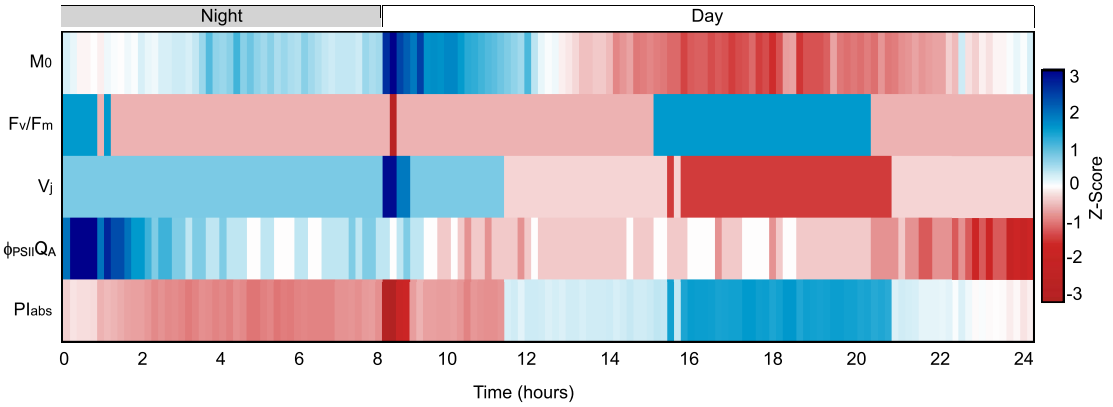

Fig. 3.6: **Heatmap of OJIP Fluorescence Parameters** Heatmap of a daily cycle (days 8 - 9) once photosynthesis has reached a steady state (as determined by relatively stable values of F_v/F_m) and *C. vulgaris* is growing in its linear phase. Values are averaged Z-Scores and demonstrate normalised increases (blue) and decreases (red) of each photosynthetic parameter. Assessments of chlorophyll *a* fluorescence were taken every 10 minutes during night (growth lights switched off) and day periods (growth lights switched on).

While values of F_v/F_m and $\phi PSIIQ_A$ are stable towards the latter part of the experimental period, PI_{abs} (performance of linear electron transport) fluctuates over the entire experimental period (Figure 3.5c). Additionally, PI_{abs}, unlike the quantum yield of PSII, decreases after ∼12 hours of growth light exposure rather than exclusively over dark periods. PI_{abs} gradually rises from a low point of 0.13 ± 0.02 after 3 hours of dilution of *C. vulgaris*. During the latter stages (>5 days) the PI_{abs} begins to drop quickly (<1 hour) upon growth light exposure, followed by a rapid reversal (<2 hours) to pre-dawn values.

To examine daily cycles in the light reactions of photosynthesis within *C. vulgaris* a heatmap was created during a stable period of photosynthetic productivity (Figure 3.6). Values are Z-scores and demonstrate relative increases and decreases in each photosynthetic parameter over a 24-hour period (days 8 - 9) starting from 8 hours of darkness. Upon the growth lights being switched off there is an increase in the quantum efficiency of PSII as seen through higher values of F_v/F_m and $\phi PSIIQ_A$. Once the growth lights are switched back on (hour 8) there is an immediate decline in PSII efficiency with higher values of PSII closure rate (M_0) and the ratio of

closed PSII reaction centres increases (V_j). PI_{abs} and F_v/F_m are reduced for a short period of time (<1 hours) before returning to ambient levels. Mid-way (hours 16-21) through the 16-hour growth light period *C. vulgaris* has higher values of PI_{abs} and F_v/F_m and lower values in M_0 and V_j. This is followed by a decrease in F_v/F_m, PI_{abs} and $\phi PSIIQ_A$ after 12 hours of growth light exposure.

3.4 Discussion

The present work has described the structure and function of the Phenobottle and demonstrated an example of its use in microalgal physiological research. The utility of the device has been shown through the Phenobottles ability to assess photosynthesis and growth accurately in *C. vulgaris* over both long (days) and short (minutes) time-scales. The use of cost-effective components and 3D printing allows the overall cost of the device to be quite low (US ∼$200 per device) compared to commercial instruments. The flow-through cuvette of the fluorometer has provided a great benefit to the overall system by providing an assessment of electron transport in photosynthesis at a near-real time resolution. The primary reason for this is that the device measures OJIP fluorescence outside of the culture flask, negating the need to illuminate the whole culture with high intensity irradiance for each chlorophyll *a* fluorescence analysis.

In the application example used here, the results indicate that electron transport in the light reactions of photosynthesis can be tracked in both an accurate and reproducible manner with parallel Phenobottles. The low and high concentration signal to noise ratio shown in Figure 3.3 provides an accurate analysis of OJIP fluorescence throughout the stationary and linear phase of growth. Issues that need to be considered when performing this kind of analysis is that the increased concentration of cells inside the fluorometer will decrease the average light intensity of the OJIP fluorometer due to the reduction in penetration depth of the actinic light [57]. To alleviate this issue, one can use turbidostat mode to keep the culture density low. In our design we have tried to minimise the effect of microalgal density by positioning

the detecting photodiode of the fluorometer as close to the emitting LED as possible. By doing so, one can avoid saturation and re-absorption of fluorescence.

Cellular concentration in solution follows a logistic function according to optical density, as there is a small lag period followed by an linear growth phase. A similar trend of growth (OD) was found in a previous study using *C. vulgaris*, with a slow phase after inoculation followed by a rapid (linear) phase and finally a stationary period over an comparable 17 day period [108]. If OD is converted to doublings of cells per day according to equation 3.2, the result is a 2^{nd} order exponential decay. This could indicate that at the start of the experimental period cellular reproduction is high due to higher irradiance (because of high transmission) and as transmission decreases the doubling time of cell density becomes longer. Other factors such as CO_2 and nutrient limitation may be contributing to this decrease which could be explored further in future experiments [109, 110].

Analysis of F_v/F_m, PI_{abs} and $\phi PSIIQ_A$ indicates that the dilution of cells at the start of the experiment places some photosynthetic stress on *C. vulgaris*. A previous study using *C. vulgaris* to determine PSII photochemistry over various growth phases yielded similar quantum yield of PSII values 3 days after inoculation (0.7 ± 0.05) compared to the Phenobottle (0.65 ± 0.03) [111]. However, [111] did not use a photobioreactor, and used a different medium (Tris-Acetate-Phosphate) and did not measure quantum yield of PSII directly after inoculation which is where we see most of the changes in photochemistry occurring. After 2 – 3 hours F_v/F_m and PI_{abs} begin to increase as *C. vulgaris* begins to acclimate to the Phenobottles.

If the fluorometer was able to assess F_v/F_m for higher cell densities, it would be expected that F_v/F_m would begin to decline as *C. vulgaris* enters its stationary phase of growth where nutrients and CO_2 and light become limiting factors. The saturation of chlorophyll *a* fluorescence measurements at high cell densities is linked with the electronics of the Phenobottle, as in this experiment the gain of the instrument was set slightly too high. To correct this issue users can adjust the sensitiivty of the Phenobottle via the electronics infrastructure. However, for other species/strains of microalgae which exhibit variable amounts of chlorophyll *a* fluorescence the user

may want to dial in the amplification of the OJIP signal to achieve the highest signal to electronic noise ratio. Alternatively, the user can operate the Phenobottle (with some minor alterations) as a turbidostat with a constant cell concentration.

The featured heatmap demonstrates the fine tuning of photosynthesis over a 24-hour period (days 8 – 9). Heatmaps have been used in previous photosynthetic studies to examine time-series data from multiple phenotypes in order to demonstrate the influence environmental variables have on photosynthetic processes [112]. The heatmap featured here has only one phenotype; however, its application demonstrates the day/night cycle of photosynthesis in *C. vulgaris* that can be expanded upon in future studies. Over 8-hours of darkness PSII photochemistry remains constant, as can be seen through little variation in F_v/F_m and PI_{abs}. However, $\phi PSIIQ_A$ increases directly after being dark inducted suggesting an immediate upturn in Q_A reduction [70]. When the growth lights are turned on, an increase in the closure rate of PSII can be seen through higher values of M_0 and V_j. This coincides with a decrease in F_v/F_m and a reduction in overall photochemistry (PI_{abs}). The day/night cycle of *C. vulgaris* is visible through a decrease in F_v/F_m, PI_{abs} and $\phi PSIIQ_A$ after 12 hours of light exposure. As *C. vulgaris* was kept in a stock culture operating at 12:12 light dark cycles, the decrease in photochemical efficiency after 12 hours suggests an adaptation to this entrained diurnal rhythm as seen in other species of microalga [113]. These data provide an accurate assessment of electron transport in microalgae at a near real-time resolution.

The Phenobottle offers a great deal of advantages over traditional culturing methods and other commercial PBR devices. Coupling growth and OJIP chlorophyll *a* fluorescence measurements in the Phenobottle makes the device a powerful tool for real-time assessments of microalgal photophysiology, which most commercial instruments are incapable of. The device is sensitive enough to capture fluctuations in photosynthesis and growth due to stresses that can go unnoticed if the user were to only use discrete (infrequent) F_v/F_m measurements. Additionally, traditional microalgal culturing methods such as Erlenmeyer flasks within an incubator, may result in heterogeneous irradiance distribution due to the flasks irregular shape and

self-shading of multiple flasks near each other. This is not an issue with the Phenobottle as the individual flat light panels and bottle shape provide a homogeneous light exposure to the entire population. The absence of mixing in some PBR systems results in self shading, with some cells receiving a lot of light and others getting very little [114]. In the Phenobottle mixing is done automatically at the users desired speed and intervals. Additionally, small features such as text message notifications when the culture reaches a certain density or if a photosynthetic parameter reaches a threshold are useful to know when to dilute a culture or to take additional external measurements. As the Phenobottle is coded in common programming languages (Python and C++), users can adapt new protocols and integrate additional sensors following the structure of pre-existing programming commands. The localhost database provides easy and quick access to current experimental data of all operational Phenobottles (Figure 3.3). Future versions of the device could implement the ability to control an array of Phenobottles from a single computer, thus allowing for faster experimental setup times.

While the Phenobottle has several benefits over some traditional PBR's, the device itself is not intended to replace commercial instruments. As shown in this experiment; if the light intensity of the chlorophyll *a* fluorometer is consistent between instruments it is possible to normalise the OJIP curves to obtain relative changes in electron transport. It is unknown to what extent instrument variation occurs between commercial photobioreactors in which to compare this limitation of the Phenobottle. Another feature that could potentially be added to the Phenobottle is further control over environmental variables including light quality (colour), temperature of the system etc.

The main benefit of a Phenobottle is in the ability to accurately assess the fine regulation of photosynthesis in microalgae. Additionally, the hardware of the Phenobottle provides uses for microalgal research through homogeneous light, mixing and bubbling for reproducible and precise microalgal research. In the future, it is foreseeable that the Phenobottle could be adapted to a wide range of innovative

methods and provide valuable information on photosynthesis, growth and functioning of various microalgal species.

4. NEAR-REAL TIME MEASUREMENTS OF PHOTOSYNTHETIC ELECTRON TRANSPORT

The previous two chapters have discussed and demonstrated the development and preliminary testing of two novel instruments. This chapter will focus on using the new devices to develop a novel and rapid technique for estimating the *absolute* rate of photosynthetic electron transport. The application of this method may prove to be a valuable tool for conducing high-throughput phenotyping using green microalga.

4.1 Introduction

Microalgae are at the forefront of biotechnological research as they may provide solutions to global issues such as food security, aquaculture feedstock, biodegradable plastics and sustainable bio-fuels [10, 115–117]. However, after decades of research there is consensus that for microalgae to become mainstream industrial solutions; two main problems need to be addressed. First, genetic tool kits for microalgae need to be developed and secondly efficient light usage in microalgal cultures must be optimised [115, 118]. While the later issue has been examined in detail, light management in photobioreactors (PBR) has been a challenging issue. This is primarily due to the fact that light penetration depth diminishes rapidly as the microalgal culture increases in concentration. As microalgae are photoautotrophic organisms, this reduction in irradiance alters the efficiency of photosynthetic processes.

A possible solution for controlling the efficiency of photosynthetic processes is to tune-up the utilization of light in PBR's by controlling microalgae's photophysiological processes. This could be achieved by regulating light absorption by light harvesting proteins (antennas) and altering electron transport between photosystems

II and I (PSII and PSI, respectively) [119]. It is vital that this process is carried out with a near-real time resolution to rapidly adjust the light conditions that the microalgae are exposed to, as a response to observed photosynthetic phenotypes.

A commonly used method of probing photosynthetic processes is through various kinds of chlorophyll *a* fluorometers. Intense excitation (in the form of irradiance) is applied to a microalgal sample resulting in the emittance of fluorescence from PSII. The fluorescence intensity is measured and interpreted based upon a quenching analysis of PSII [58]. Several parameters resulting from chlorophyll *a* fluorescence have been proposed to probe photosynthetic efficiency such as: the maximum quantum yield of primary photochemistry (ϕ_{Po}, also known as F_v/F_m); the photosynthetic electron transport rate of PSII (ETR_{II}), an indicator of how efficiently electrons move through the electron transport chain and generate reducing power; or the absorption cross section of PSII (σ_λ, which indicates the efficiency in wavelength absorption by photosynthetic antenna [61, 71]. While ETR_{II} and σ_λ are very useful parameters, they are time consuming to measure, require advanced instrumentation and therefore are not suitable to monitor photosynthetic processes in real-time. Alternatively, ϕ_{Po} is quite fast to measure (< 1 s); however, this parameter only changes when catastrophic stress events in photosynthetic organisms occur.

A major obstacle in optimising microalgal production is linked to the fact that a real-time, rapid assessment of photosynthetic electron transport in microalgae does not exist. To overcome this issue, we report a new method to estimate ETR_{II} at a near-real time resolution, utilizing the seconds-time-domain-component of the polyphasic fluorescence induction curve of chlorophyll *a* (colloquially referred as OJIP). To test this approach, we cultivated the green microalga *Chlorella vulgaris* under three different lighting qualities (Red-Green-Blue (RGB), Red-Blue (RB) and Warm White (White) LEDs) using identical irradiance and in-house designed, 3D-printed, open-source photobioreactors known as Phenobottles [102]. Continuous (every ten minutes) optical density and OJIP measurements were accompanied by ETR_{II}, pH and σ_λ calculations at discrete intervals (termed pre-dawn, dawn, mid-day, afternoon and night). The trial is then repeated by utilising derived parameters

to modulate both the growth rate and maximum photosynthetic ETR_{II} of *C. vulgaris*.

4.2 Materials and Methods

4.2.1 Microalgal Species

The green microalgal *Chlorella vulgaris* (UTS-LD) (Phylum Chlorophyta) was chosen as the test species based upon recent work describing its potential for the production of sustainable bio-fuels, as a food source for aquaculture and the treatment of waste-water [115, 116]. At the time of sub-culturing *C. vulgaris* was growing in its exponential phase in MLA media with 60 μmol photons m^{-2} s^{-1} of RGB LED light (measured using a 2π PAR meter (LI-250A, LiCor, Nebraska, USA)) on 12-12 hour light-dark cycles in a Phenobottle [82].

4.2.2 Photobioreactor and Light Arrangement

Open-source, 3D printed PBR's known as Phenobottles were constructed and employed to assess photosynthesis and growth of *C. vulgaris* (Figure 4.1). These PBR's are based around 75 cm^2 culture flasks, have automated mixing, bubbling of air and their own growth light configuration. Growth lights were constructed in three different arrangements: (1) Warm White (5050 SMD), (2) Red-Blue-Green (RGB) (5060 SMD) and (3) Red-Blue (RB) (5060 SMD) and calibrated to an irradiance of 60 μmol photons m^{-2} s^{-1} using a 2π PAR meter.

4.2.3 Automated Measurements

Phenobottles are equipped with individual, open-source, in-house made, 626 nm OJIP chlorophyll *a* fluorometers [57]. OJIP chlorophyll *a* fluorescence is based upon an analysis of quenching resulting from PSII [80]. This method uses dark-adapted photosynthetic microalga which are then exposed to a flash (>1 second in duration) of continuous irradiance. A detector, shrouded by a long pass filter (>695 nm),

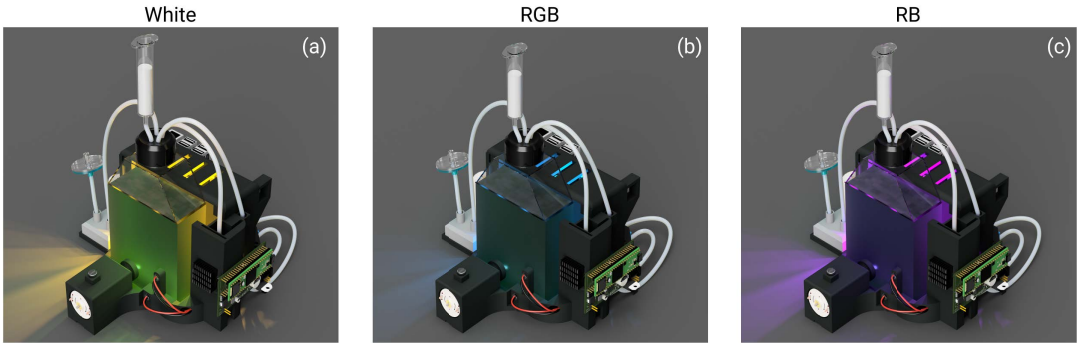

Fig. 4.1: **3D render of the Phenobottle lighting arrangements used.** White Light (a); RGB (b) and RB (c) arrangements are shown as a representation of the light quality implemented to target the optimal absorption cross section of PSII.

measures the resulting chlorophyll *a* fluorescence signature, composed of distinct three phases; O-J, J-I and I-P [59, 64]. Every 10 minutes 5 mL of *C. vulgaris* was automatically extracted from the culture flask by a peristaltic pump into the integrated cuvette OJIP fluorometer for dark-adaptation and analysis before being pumped back into the main growth culture flask for re-homogenisation.

Each Phenobottle is fitted with an automated 875 nm optical density (OD_{875}) sensor located between the main culture flask (38 mm path length) which is used as a proxy of cell concentration.

4.2.4 External Manual Measurements

A multiple wavelength chlorophyll *a* fluorometer (MC-PAM, Heinz Walz GmbH, Germany) was employed to perform an analysis of chlorophyll *a* fluorescence quenching to complement the in-bottle OJIP measurements [61]. 1.5 mL of *C. vulgaris* was extracted from each Phenobottle through intravenous-connectors (BD Q-SyteTM, BD, New Jersey, USA) at discrete time-points throughout a daily growth cycle. The sample was then added drop-wise into a quartz cuvette (10 mm path length) until a pre-optimised fluorescence reading was achieved in the MC-PAM.

The optical wavelength-dependent absorption cross section of PSII (σ_λ) of *C. vulgaris* was calculated at five-wavelengths (440, 480, 540, 590 and 625 nm) using multiple short (1 ms) continuous flashes of actinic light (AL), followed by a 50

μs single turnover saturation pulse. The resulting induction curve of chlorophyll *a* fluorescence (known as an O-I_1 rise) was fitted (using PamWin3 Software) for each wavelength as described by [61]. The derived parameters from the O-I_1 rise were used to calculate σ_λ (4.1). Where $k(II)$ is the rate constant of PSII turnover (1 ms^{-1}), τ (Tau) is a time constant of Q_A (a primary electron acceptor of PSII) reduction and L is Avogadro's constant.

$$\sigma_{II}(\lambda) = \frac{k(II)}{\tau \times PAR \times L} = \frac{1}{\tau \times PAR \times L} \tag{4.1}$$

Following σ_λ assessment, a light response curve (LC) using the MC-PAM at an excitation wavelength matching that of the OJIP fluorometer (626 nm) was preformed [61]. The LC routine was set to 30 seconds between each increasing irradiance step for a total number of 20 steps from 0 – 1,995 μmol photons m^{-2} s^{-1}. The resulting derived parameters were combined with σ_λ estimations to calculate the photon absorption rate of PSII (PAR_{II}) and the *absolute* electron transport rate originating from PSII (ETR_{II}).

$$PAR_{II} = \sigma_{II}(\lambda) \times L \times PAR \tag{4.2}$$

$$ETR_{II} = PAR_{II} \times \frac{Y(II)}{Y(II)_{MAX}} \tag{4.3}$$

Where $Y(II)$ is the effective quantum yield of PSII, and $Y(II)_{MAX}$ is the maximum quantum yield of photosynthesis (also known as ϕ_{Po}).

4.2.5 Rapid Electron Transport Rate Assessment

To associate continuous OJIP fluorescence transients with discrete ETR_{II} estimations, a normalisation was applied to each OJIP transient from F_o, representing the minimum level fluorescence to F_m, the maximum fluorescence intensity, represent-

ing an oxidised and reduced electron transport chain, respectively. The normalised fluorescence intensity at time (t) can then be derived using Equation 4.4.

$$FN_t = \frac{F_t - F_o}{F_m - F_o} \tag{4.4}$$

Normalisation is required to compare OJIP measurements from different photobioreactors and nullify the effects of increasing culture densities as *C. vulgaris* cells replicate over time.

4.2.6 Experimental Design

Phenobottles were set to a 12-12 hour light:dark cycles in a 21°C temperature-controlled room. Each Phenobottle was filled with 200 mL of MLA media, supplemented with 40 mL of stock culture *C. vulgaris* through an intravenous-connector and given four days to stabilise before starting the experiment [82]. All treatments were then diluted with MLA media to a time zero OD_{875} of ∼0.2. Over the course of 16 hours, five external measurements were taken at discrete time-points (pre-dawn, dawn, midday, afternoon and night) and complemented by continuous (every 10 minutes) internal measurements of both OD_{875} and OJIP chlorophyll *a* fluorescence. The trial was repeated five days later; however, this time the RB light culture was altered to have a reduced growth light intensity of 44 μmol photons m^{-2} s^{-1} in order to modulate ETR_{II}.

4.3 Results

We used three separate photobioreactor growth light arrangements (at the same PAR intensity) to modify and probe photophysiology in the microalga *C. vulgaris* (Figure 4.1). The normalised spectral output of the growth lights for each treatment are displayed in Figure 4.2 with a PAR overlay as a qualitative indicator of the growth light quality at each wavelength. There are visible differences in σ_λ for each

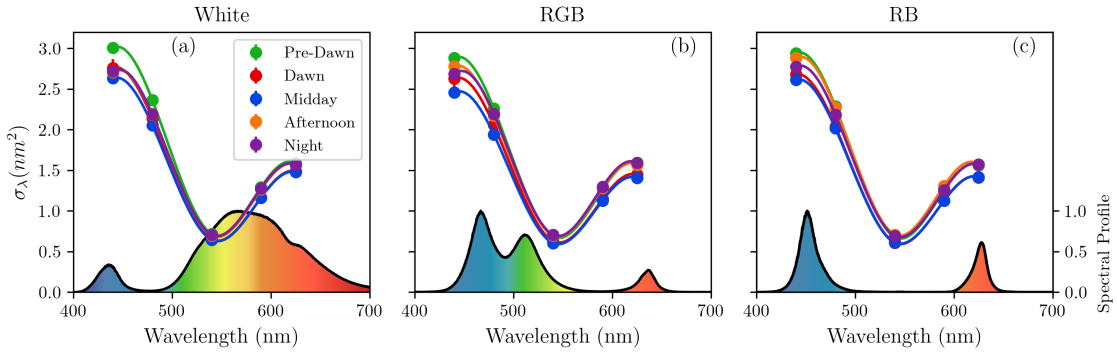

Fig. 4.2: **σ_λ calculations across a daily growth cycle.** Parts (a), (b) and (c) denote the growth light spectra used, White, RGB and RB, respectively. Five wavelengths (440, 480, 540, 590 and 625 nm) were used to estimate the wavelength dependent antenna size of PSII (σ_λ). A cubic line interpolation was fitted to better demonstrate changes in σ_λ. σ_λ calculations are averages (n = 3) ± SD. A false colour map (PAR spectra) has been overlaid in a – c to demonstrate the spectral profile of each treatment.

treatment, with σ_{440nm} having the greatest effective antenna size of ∼2.8 nm^2 and σ_{540nm} being the smallest at ∼0.75 nm^2.

Optical density (OD_{875}) measurements were employed in each Phenobottle as a proxy of cell concentration using automated 10-minute intervals (Figure 4.3). Figure 4.3a demonstrates the effect of light quality on the growth rate of *C. vulgaris* at identical PAR irradiances. RB growth irradiance had significantly increased growth rates ($OD_{875}(MAX) = 0.156 \pm 0.004$) when compared to White and RGB treatments (of 0.115 ± 0.006 and 0.110 ± 0.002, respectively). Figure 4.3b depicts the OD_{875} of *C. vulgaris* after modulating the RB treatment to a PAR intensity of 44 μmol photons m^{-2} s^{-1}. RB light had the highest OD_{875} out of the three treatments with an OD_{875} of 0.119 ± 0.005. RGB and White light again follows similar trajectories of growth with slightly lower maximum OD_{875} values of 0.107 ± 0.005 and 0.103 ± 0.009.

OD_{875} measurements were carried out continuously with accompanying OJIP fluorescence measurements using a 625 nm open-source, in-house built chlorophyll *a* fluorometer known as Open-JIP [57]. The fluorometer is positioned outside the main growth vessel of the photobioreactors, thus allowing for independent dark-

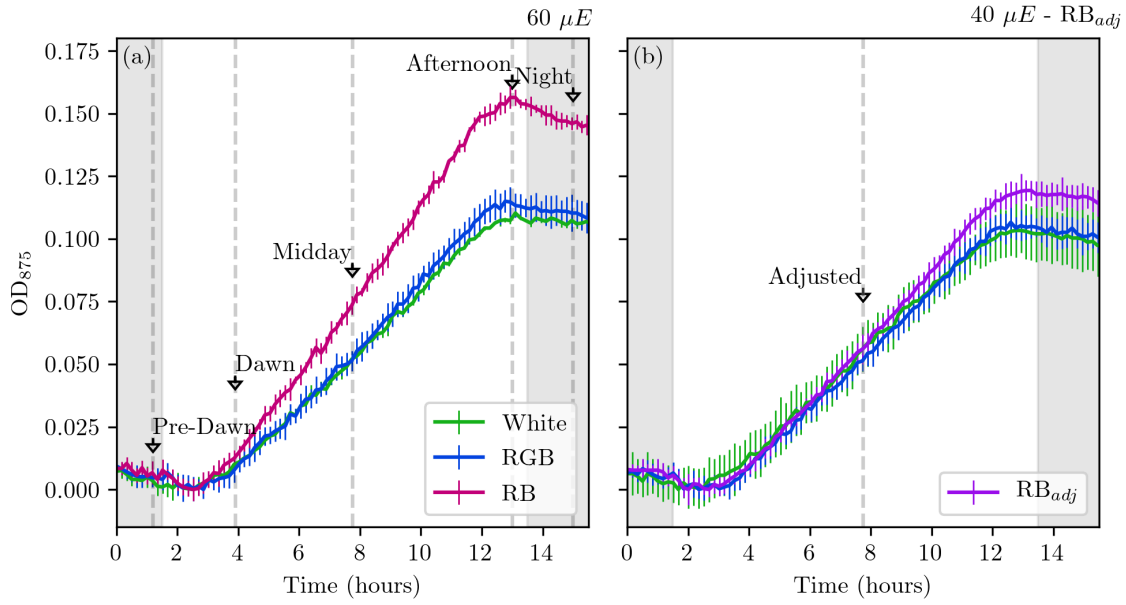

Fig. 4.3: **OD_{875} calculations before (a) and after (b) ETR_{II} adjustment.** (A) Normalised OD_{875} measurements every ten minutes over the first ~16-hour experimental period. Light intensity within each Phenobottle is set to 60 μmol photons m^{-2} s^{-1}. (B) Normalised OD_{875} measurements over the second 16-hour period after recalibrating the RB light treatment growth light intensity to 44 μmol photons m^{-2} s^{-1}. Both (A) and (B) are normalised to zero to demonstrate relative changes in OD_{875}. Data are averages (n = 3) ± SD.

adaptation of a sub-sample and rapid OJIP inductions without needing to dark-adapt the entire culture vessel. The fluorometer provides near real-time estimations of ϕ_{Po}, as well as the entire induction curve of chlorophyll *a* fluorescence (Figure 4.4a). ϕ_{Po} calculations demonstrate a steady increase in all treatments from ~0.655 to ~0.68 over the experimental period.

pH was measured at discrete intervals as a surrogate CO_2 sensor (Figure 4.4b). Each treatment resulted in a gradual increase in pH over the experimental period. Pre-Dawn values were the lowest for all treatments (White=8.8 ± 0.02, RGB=9.04 ± 0.14, RB=9.16 ± 0.14). pH rises until the Afternoon, whereby all treatments reached a peak alkalinity (White=10.01 ± 0.02, RGB=10.16 ± 0.05, RB=10.38 ± 0.02). The Afternoon peak is followed by a rapid reduction in pH after the growth lights are switched off (White=9.56 ± 0.08, RGB=9.86 ± 0.04, RB=10.01 ± 0.10).

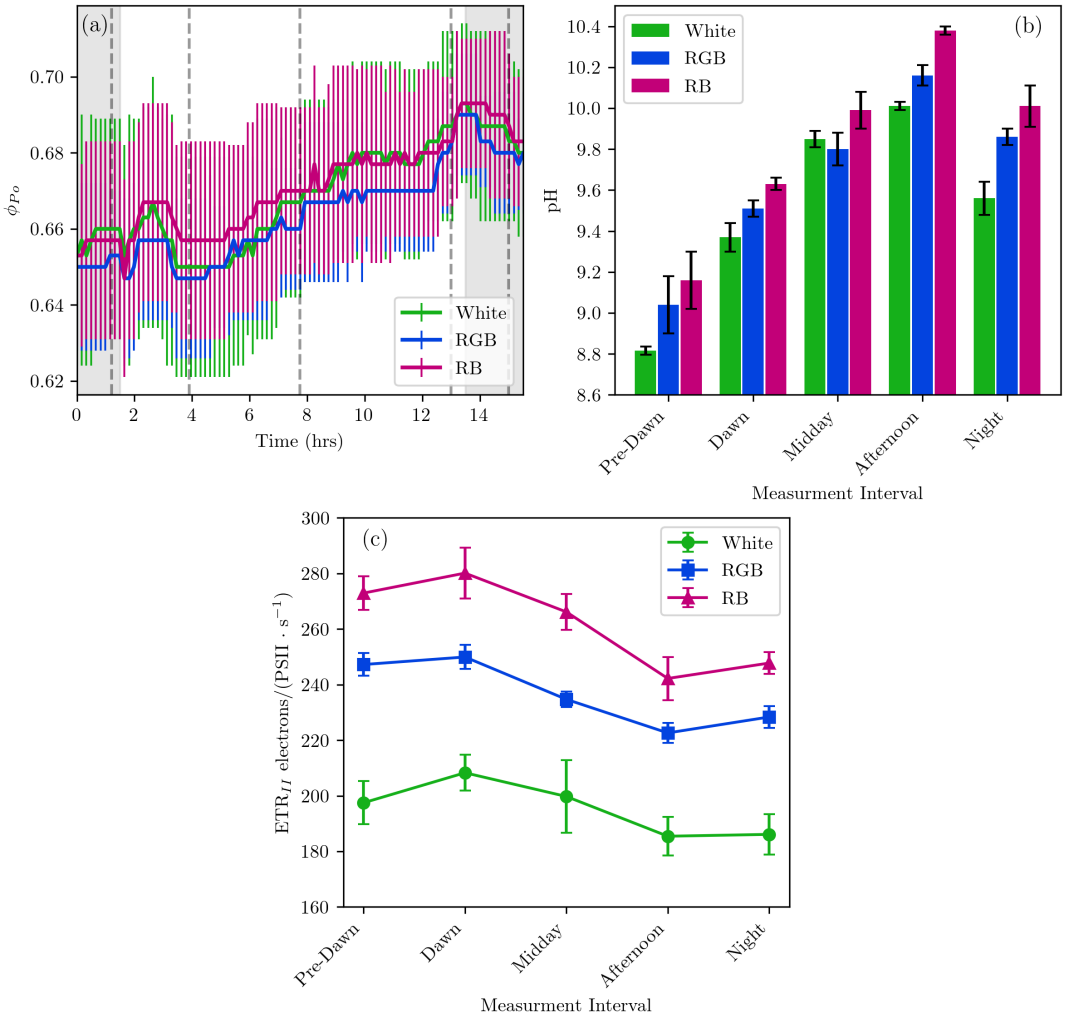

Fig. 4.4: **Changes in photosynthetic parameters over a daily growth cycle.** (A) Continuous ϕ_{Po} measurements using OJIP fluorescence. Dark bars represent times at which the growth lights are switched off. Vertical lines represent external sampling times. (B) pH changes in each treatment at discrete intervals. (C) Maximum ETR_{II} measurements at discrete intervals as determined by LC analysis. Colours represent treatment used (White = Green, RGB = Blue, RB = Magenta). Data are averages (n = 3) ± SD.

ETR_{II} calculations were determined at discrete intervals using a multi-wavelength chlorophyll *a* fluorometer by first determining the σ_λ (Figure 4.2) and then preforming a 10-minute light induction curve (LC) at 625 nm (Figure 4.4). Dawn was the highest achieved electron transport rate for all treatments (White=208.3 ± 6.5, RGB=249.9 ± 4.3, RB=280.1 ± 9.2). The greater the maximal value of ETR_{II}, the greater the drop in ETR_{II} as the day progressed, as demonstrated by the difference

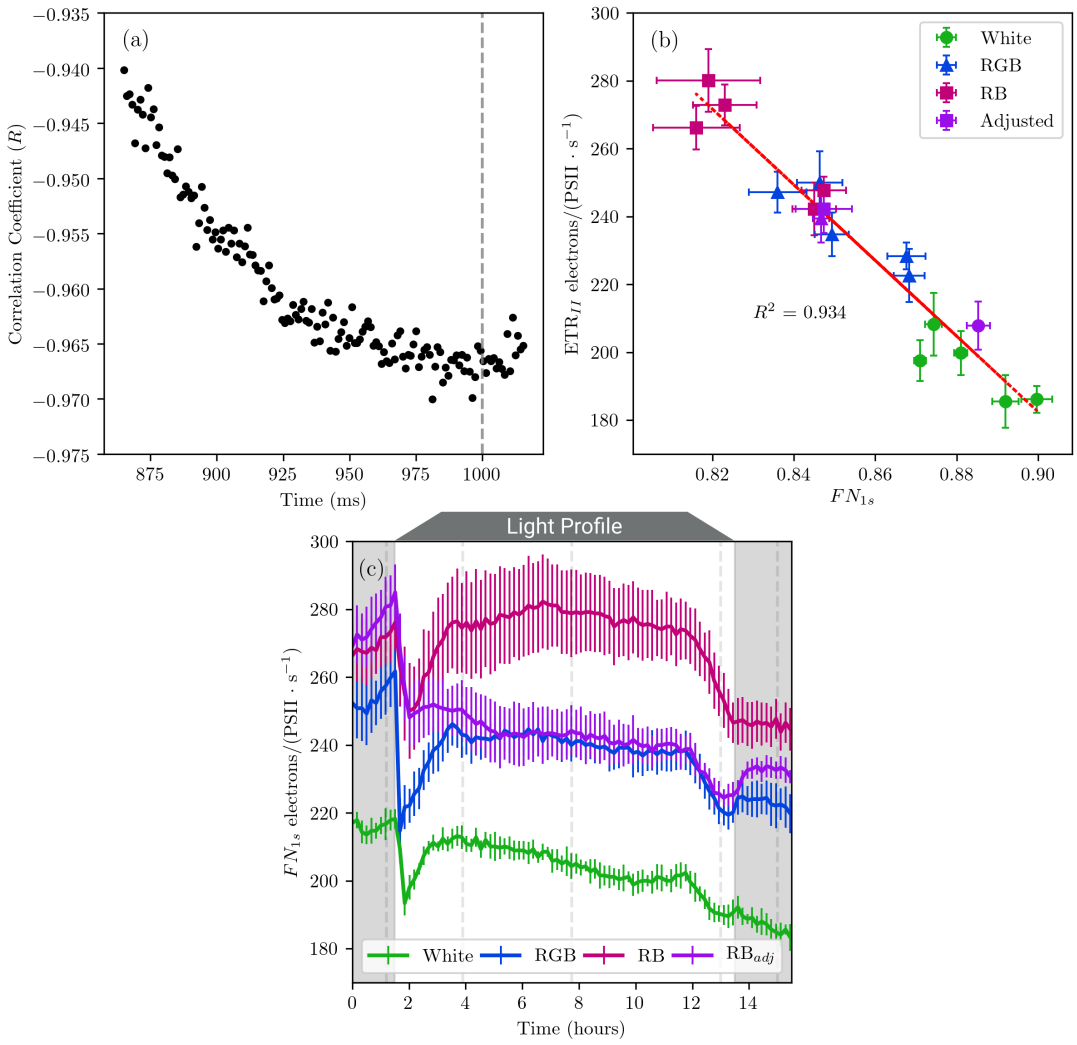

Fig. 4.5: **Optimisation and calculation of real-time** ETR_{II} (a) Correlation coefficient (R) optimisation of ETR_{II} vs FN_t, where t equals a time-point in the OJIP fluorescence induction curve between 850 to 1015 ms. Vertical dashed line is used to represent the location of FN_{1s}. (b) FN_{1s} vs ETR_{II} at discrete time points fitted to a linear regression ($R^2 = 0.934$). (c) Estimates of maximum ETR_{II} using continuous fluorescence transients (10-minute intervals) (FN_{1s}). Colours represent growth light irradiance used (White = Green, RGB = Blue, RB = Magenta, RB_{adj} = Purple). RB_{adj} shown in (c) demonstrates the estimated maximum ETR_{II} of *C. vulgaris* after adjusting light intensity in the Phenobottle to 44 μmol photons m^{-2} s^{-1}. Dark bars represent time when the growth lights are switched off. Insert above (c) depicts the growth light profile used for all Phenobottles. Data are averages (n=3) ± SD.

between the maximum and minimum values of ETR_{II} (White=22.8, RGB=27.3, RB=37.9).

The amplitude of normalized fluorescence intensity of one second after the AL light was switch on (FN_{1s}) in the OJIP fluorometer was used as a proxy of near-real time maximum ETR_{II}. One second was chosen based upon the optimization of correlation coefficient (R) calculations between maximum ETR_{II} and the normalized fluorescence intensity (FN_t) from 850 – 1015 ms at discrete time-points (Figure 4.5a). These time-points were chosen as they occur after F_m and best demonstrate a peak correlation occurring at 1000 ms. Normalized values were used to negate the growth of *C. vulgaris* effecting OJIP transients and to ensure measurements between OJIP fluorometers are alike. Correlation coefficient values demonstrate a gradual increase in a negative correlation between ETR_{II} and FN_t. The displayed coefficient values decrease from -0.940 to a terminal correlation of ∼-0.968 occurring at ∼1 second, hereafter R values begin to increase.

The optimized linear relationship between FN_{1s} and ETR_{II} is demonstrated in Figure 4.5b. There are six discrete measurements displayed representing various time-points throughout the experimental period both before and after altering the growth light irradiance in the RB treatment (RB_{adj}) (Figure 4.3). Calculations of FN_{1s} and ETR_{II} are inverse, as greater normalized fluorescence intensity represents higher quenching due to a blockage of electrons in the photosynthetic electron transport chain. Therefore, lower values of FN_{1s} indicate increased photosynthetic electron transport.

Using the linear regression depicted in Figure 4.5b, a near-real time (10-minute intervals) assessment of maximum ETR_{II} can be calculated from continuous OJIP transient probes (Figure 4.5c). FN_{1s} follows that of the growth light arrangement used with a two-hour increase and decrease in light intensity at the start and end of the growth light period. RB_{adj} represents the maximal ETR_{II} of *C. vulgaris* over the experimental period after adjusting the growth light intensity to alter ETR_{II} and therefore growth (Figure 4.3).

4.4 Discussion

In this work, a method to rapidly assess electron transport rates on the bases of photon absorption by PSII (ETR_{II}) was presented (termed FN_{1s}). The method consists of a predictive model constructed from actual ETR_{II} measurements performed using conventional pulse amplitude modulation (PAM) fluorometry to derive a novel parameter from the fast polyphasic rise of chlorophyll *a* fluorescence (OJIP) curve. FN_{1s} is estimated by double normalizing OJIP induction curves and parametrizing the fluorescence intensity at one second. Due to its fast estimation (few seconds) and capacity to be probed frequently (every 10 minutes), FN_{1s} offers near real-time assessment of the *absolute* maximum photosynthetic electron transport rate originating from PSII.

σ_λ calculations indicates that changes in spectral quality does not influence antenna composition over short time scales (days) as each treatment has shown an identical overall trend (Figure 4.2). A reduction of PSII antenna size has been shown to increase the productivity of *C. vulgaris* [119]. However, this was preformed using a higher light intensity (>200 μmol photons m^{-2} s^{-1}), which results in an environment where light is in excess. Here however, the focusing of light intensity to the optimal optical cross section of PSII at a lower light intensities (such as within photobioreactors where self-shading is a major issue) were aimed to adjust the productivity (growth rate) of *C. vulgaris*.

Ideally, an advanced analysis of photosynthetic processes should be conducted *in-situ*, continuously and in a non-invasive manner. The most widely used method of rapid photosynthetic performance indication is ϕ_{Po}. However, ϕ_{Po} does not represent the actual photosynthetic electron flux and does not recognize observed changes of photosynthetic performance across a single light cycle. An evaluation of ETR_{II} is more applicable, as it provides the *absolute* rate of electron transport and takes into account the antenna size of PSII [61]. The issue with ETR_{II} measurements is that they are time-consuming, require advanced instrumentation and disrupt the photophysiology of the microalgae due to their long excitation exposures.

The method used here is based on similar concepts to that which is proposed when performing OJIP chlorophyll *a* fluorescence analysis. In this kind of analysis, darkness is used as a reproducible reference state as the photosynthetic electron transport chain becomes fully oxidized due to a lack of excitation energy. Here we propose that FN_{1s} works in the same way, except the reproducible reference state is a fully *reduced* electron transport chain occurring at the P-step (F_m). The drop in fluorescence intensity from the P-step to FN_{1s} is related to electron transport through the electron transport chain. As a result of this, reduced electron transport results in higher fluorescence intensity (higher values of FN_{1s}) and increased ETR_{II} results in decreased fluorescence intensity (lower values of FN_{1s}).

Previous work on the extended phases (beyond F_m or P) of OJIP fluorescence in isolated chloroplasts (from pea leaves) are correlated with energy dependent quenching (qE), which represents energy dissipation triggered by the formation of a ΔpH gradient between the thylakoid lumen and stroma [120, 121]. As the formation of a ΔpH gradient occurs concomitantly with electron transport through proton translocation across the thylakoid membrane, a relationship between the extended OJIP phases shown here is aligned with the findings of this work.

The thermal phases of the polyphasic rise of chlorophyll *a* fluorescence are not as well defined as the photochemical steps as they are affected by multiple processes [64]. As such the thermal (slow) phase defines a *range* of time where these phases may occur. The new parameter (FN_{1s}) describes a *specific* point in time that relates to the *absolute* electron transport rate of that microalga. This point in time may change between species and as such may be calculated through equation 4.4 to derive a specific calibration for different species.

Commonly used photosynthetic probes are either too slow, too technically complex or do not represent the entire light dependent reactions of photosynthesis. The method devised here can be used as a rapid indicator of ETR_{II} regardless of the growth light source color and takes into account the antenna size of PSII (σ_λ). However, the derived parameter (FN_{1s}) is unit-less unless combined with conventional ETR_{II} and σ_λ measurements as shown here. Nonetheless, the technique can be

used as a relative indicator of maximum ETR_{II}. This technique could be applied to create feedback mechanisms for optimising microalgae productivity in cultivators. Alternatively, the rapid probing technique may be useful for microalgal physiological research as a sensitive indicator of photosynthetic processes in green microalgae.

5. SYNTHESIS

5.1 Summary of Thesis

The devices and methods presented in this thesis are aimed at increasing the capacity of microalgal research to progress towards expansive and data-rich experimental designs. Each device was constructed in a cost effective manner and are completely open-source, allowing researchers with varying budgets to download and implement the devices to suit their own experimental requirements.

The chlorophyll *a* fluorometer presented in Chapter 2 (Open-JIP) can be used as shown in Chapter 3 to assess photosynthetic phenotypes in real-time. Alternatively, the device can be used as a stand-alone fluorometer for assessing the photosynthetic properties of microalgae or plants that are used in other biological disciplines. Altering the device into a USB powered multi-wavelength desktop chlorophyll *a* fluorometer with a simple user interface could increase its usefulness for microalgal research by allowing researchers who are not comfortable with using the command-line to to control the device. Additionally, the plant version of Open-JIP could be modified into a battery powered system to use in the field, without the need for a computer. These simple devices are also interesting candidates for teaching students and community members about photosynthesis and how they can design their own instrumentation to solve problems in other areas of scientific research.

The Open-JIP fluorometer does poses the ability to be adapted to some novel environmental probes. A particularly interesting application of the fluorometer is in the field of plant phenomics. Here plant scientists are trying to create a map of a particular species response to environmental conditions to enhance the productivity of crops. Commonly, greenhouses are implemented to control environmental

conditions while physiology is probed in an autonomous manner (using robots or scanning techniques). However, the Open-JIP device could be adapted as a low-cost phenomics device in the field by using imaging software to identify the plant (take an image and compare it to a database of images of various plants so see which matches the best). The user then takes a measurement using the device which captures both the photosynthetic phenotype of the plant and the associated environmental conditions (through environmental sensors; temperature, CO_2 etc.). The information is sent to a database of previous measurements to compare and create a map of phenotype-environment interactions for that species. The data acquired over time may contain phenotype-environment interactions of various genotypes without the need for expensive phenotyping greenhouses.

Chlorophyll *a* fluorescence as a technique has been used for over halve a century. However, the application of the technique outside of research circles has not been realised. This may be due to the complex nature of the technique and its interpretation, the unclear nature between measurements and their application for hobbyists or the price of the instrumentation. The Open-JIP device may represent a linkage between research circles and the broader community. The device could be implemented as a low-cost sensor with time series data collection for citizen scientists. The use of time-series data may provide the link between the devices acquisitions and the real-world implications for users. For example, a gradual decline in F_v/F_m may represent a decline in productivity and therefore intervention measures needs to be conduced to amend these issues (more water, increase shade cover etc.).

The Phenobottles featured in Chapters 3 and 4 of this thesis are capable of reproducible experimental procedures and can accurately track photosynthesis and productivity in a near-real time manner. Current methods of cultivating microalgae for research is still contained within incubators where a number of issues such as self-shading, absence of mixing, heterogeneous light etc. all become uncontrolled variables. The Phenobottles design is aimed at making the device as low-cost as possible without sacrificing accuracy and usability to increase the number of researchers using photobioreactors to control these factors. Additionally, Phenobottles provide

researchers with the ability to perform all experimental replicates and treatments at once (using an array of devices) rather than using one or two high-cost devices in a serial manner. Additionally, the Phenobottle has only been tested upon a single green alga species. Therefore, the application of other microalga Phyla may provide interesting results for increasing the productivity of these organisms or maximising the production of valuable bio-compounds.

The novel method presented in Chapter 4 of measuring ETR_{II} in a near-real time manner is extremely useful for physiological research. Using this method researchers can estimate the rate of photosynthetic electron transport using a rapid (one second) measurement, rather than a >20 minute procedure using advanced instrumentation. Other methods such as ϕ_{Po} calculations have proven to be too invariable for assessing the fine tuning of photosynthesis, as such this new method may provide a more accurate representation of how the entire electron transport chain is functioning. The rapid ETR_{II} measurements could be used as a feedback mechanism to the photobioreactors environmental settings (particularly light intensity) to accurately modulate electron transport. Additionally, the technique of focusing light quality to the antenna composition of *C. vulgaris* in Chapter 4 has proven to be a useful method of increasing the productivity of the microalga while reducing the amount of wasted irradiance by poorly absorbed wavelengths. This technique could prove useful for maximising light utilisation when applied to other species of microalga with various antenna compositions and state-transitions (such as cyanobacteria).

5.2 A Perspective on the Future of Microalgal Physiological Research

Microalgae have been studied for many decades with no clear indication that the problems faced when industrially producing microalgae can be overcome. Current methods of conducting microalgal physiological research aim to build upon previous research in order to understand physiological responses of microalgae to environmental variables. However, the issue with this approach is that each study is performed

using various and often undefined environmental conditions which results in unclear phenotype-environment interactions.

Frequently environmental conditions in microalgal physiological research are 1) defined by the researchers, but only demonstrate a subset of the total number of environmental variables; 2) defined by the researchers but the techniques used to measure the environmental conditions are inconsistent or 3) the environmental conditions are undefined by the researchers. For example, light quality is an important factor in microalgal physiological research as demonstrated in Chapter 4 (Figure 4.3). However, light quality is often ignored, which results in studies using fluorescent bulbs, LED's etc. to resolve phenotypic responses. As an expressed phenotype is as a result of an organisms life history, genotype and the environment, the observed phenotype is confined to the studies environmental profile [25]. This may result in conflicting models which are discussed for many years, several of which may be true, but not because of varying mechanisms, but rather varying phenotypic expression (due to undefined environmental variability between the conflicting models). An alternative method of conducting microalgal research involves a holistic approach that focuses on the end goals of physiological research (increased productivity, increased valuable bio-compound yields etc.).

The photobioreactor (Phenobottle) featured in Chapter 3 of this thesis could be capable of conducting holistic experiments for microalgal physiological research with some upgrades. These vital upgrades include physiological sensors (pH probe, O_2 sensor, spectrometer etc.) and environmental controls (temperature, media composition etc.). Once the hardware of the Phenobottle has been advanced to a state where both physiological processes and environmental conditions can be accurately measured and controlled by the software of the Phenobottle. Here the researcher must define the *parameter of optimisation* (the end goal) which can be any physiological trait that the microalga possesses that can be probed in a rapid and non-invasive manner (i.e. optical density (growth), lipid content (cell size) etc.). Once defined, the Phenobottle needs to respond to the microalga's expressed phenotypes to adjust environmental variables in order to enhance the *parameter of optimisation*. This

requires the Phenobottle to understand phenotype-environment interactions which is only possible through the use of a neural network. Specifically, a recurrent neural network (RNN) could be implemented as a feedback mechanism between the microalga's physiology and the environmental conditions that the phenotype is expressed in. As neural networks require a large number of iterations to *learn* how systems function, the Phenobottles low-cost becomes an important factor as an array of identical devices will be required. Over time, the Phenobottles will develop an understanding of what expressed phenotype requires what environmental condition and will change the Phenobottles environmental state accordingly. The end goal being that the microalgae are the ones that control the photobioreactors environment (unknowingly) through their expressed phenotypes.

5.3 Concluding Remarks

This thesis has demonstrated the development and implementation of novel tools for microalgal research. These devices can be constructed at a low-cost without sacrificing accuracy, allowing for expansive and reproducible experimental designs. All presented instruments are completely open-source and customisable to suit the researchers specific experimental requirements. Additionally, the instruments have shown to be a valuable asset in attaining a deep analysis of photosynthesis within microalgae. Open-JIP and The Phenobottle provide a foundation for future studies to explore microalgaes biotechnological potential. This may be achieved though the alternative techniques of conducting physiological research as put forward in Chapter 5 or by using the devices in an alternative manner. The culmination of this may lead microalgal research toward the creation of sustainable biotechnological industries of the future.

REFERENCES

1. Lee, R. E. *Phycology* (Cambridge university press, 2008).
2. Guiry, M. D. How many species of algae are there? *Journal of phycology* **48,** 1057–1063 (2012).
3. Burkholder, P. R. & Mandelli, E. F. Productivity of microalgae in Antarctic sea ice. *Science* **149,** 872–874 (1965).
4. Castenholz, R. W. The effect of sulfide on the blue-green algae of hot springs II. Yellowstone National Park. *Microbial Ecology* **3,** 79–105 (1977).
5. MacLulich, J. H. Colonization of bare rock surfaces by microflora in a rocky intertidal habitat. *Mar Ecol Prog Ser* **32,** 91–6 (1986).
6. Yuan, X., Xiao, S. & Taylor, T. N. Lichen-like symbiosis 600 million years ago. *Science* **308,** 1017–1020 (2005).
7. Borowitzka, M. A. Microalgae for aquaculture: opportunities and constraints. *Journal of applied phycology* **9,** 393 (1997).
8. Abdel-Raouf, N., Al-Homaidan, A. & Ibraheem, I. Microalgae and wastewater treatment. *Saudi journal of biological sciences* **19,** 257–275 (2012).
9. Lam, M. K. & Lee, K. T. Microalgae biofuels: a critical review of issues, problems and the way forward. *Biotechnology advances* **30,** 673–690 (2012).
10. Price, S., Kuzhiumparambil, U., Pernice, M. & Ralph, P. J. Cyanobacterial Polyhydroxybutyrate for Sustainable Bioplastic Production: Critical Review and Perspectives. *Journal of Environmental Chemical Engineering,* 104007 (2020).
11. Ramaraj, R., Tsai, D. D.-W. & Chen, P. H. Freshwater microalgae niche of air carbon dioxide mitigation. *Ecological engineering* **68,** 47–52 (2014).
12. Singh, U. B. & Ahluwalia, A. Microalgae: a promising tool for carbon sequestration. *Mitigation and Adaptation Strategies for Global Change* **18,** 73–95 (2013).
13. Beardall, J. & Raven, J. A. The potential effects of global climate change on microalgal photosynthesis, growth and ecology. *Phycologia* **43,** 26–40 (2004).

14. Moreira, D. & Pires, J. C. Atmospheric CO2 capture by algae: negative carbon dioxide emission path. *Bioresource technology* **215,** 371–379 (2016).

15. Safi, C., Zebib, B., Merah, O., Pontalier, P.-Y. & Vaca-Garcia, C. Morphology, composition, production, processing and applications of Chlorella vulgaris: A review. *Renewable and Sustainable Energy Reviews* **35,** 265–278 (2014).

16. Yamamoto, M., Fujishita, M., Hirata, A. & Kawano, S. Regeneration and maturation of daughter cell walls in the autospore-forming green alga Chlorella vulgaris (Chlorophyta, Trebouxiophyceae). *Journal of Plant Research* **117,** 257–264 (2004).

17. Lim, S.-L., Chu, W.-L. & Phang, S.-M. Use of Chlorella vulgaris for bioremediation of textile wastewater. *Bioresource technology* **101,** 7314–7322 (2010).

18. Liu, Z.-Y., Wang, G.-C. & Zhou, B.-C. Effect of iron on growth and lipid accumulation in Chlorella vulgaris. *Bioresource technology* **99,** 4717–4722 (2008).

19. Fradique, M. *et al.* Incorporation of Chlorella vulgaris and Spirulina maxima biomass in pasta products. Part 1: Preparation and evaluation. *Journal of the Science of Food and Agriculture* **90,** 1656–1664 (2010).

20. Palenik, B. *et al.* The genome of a motile marine Synechococcus. *Nature* **424,** 1037–1042 (2003).

21. Robertson, B. R., Tezuka, N. & Watanabe, M. M. Phylogenetic analyses of Synechococcus strains (cyanobacteria) using sequences of 16S rDNA and part of the phycocyanin operon reveal multiple evolutionary lines and reflect phycobilin content. *International journal of systematic and evolutionary microbiology* **51,** 861–871 (2001).

22. Wilmotte, A. & Stam, W. T. Genetic relationships among cyanobacterial strains originally designated as 'Anacystis nidulans' and some other Synechococcus strains. *Microbiology* **130,** 2737–2740 (1984).

23. Macias-Sanchez, M. *et al.* Supercritical fluid extraction of carotenoids and chlorophyll a from Synechococcus sp. *The Journal of Supercritical Fluids* **39,** 323–329 (2007).

24. Gross, S. *et al.* Optimization of a high-throughput phenotyping method for chain-forming phytoplankton species. *Limnology and Oceanography: Methods* **16,** 57–67 (2018).

25. Houle, D., Govindaraju, D. R. & Omholt, S. Phenomics: the next challenge. *Nature reviews genetics* **11,** 855–866 (2010).

26. Davis, B. D. The isolation of biochemically deficient mutants of bacteria by means of penicillin. *Proceedings of the National Academy of Sciences of the United States of America* **35,** 1 (1949).

27. Bernard, O. & Rémond, B. Validation of a simple model accounting for light and temperature effect on microalgal growth. *Bioresource technology* **123,** 520–527 (2012).

28. Lewis, M. R. & Smith, J. C. A small volume, short-incubation-time method for measurement of photosynthesis as a function of incident irradiance. *Marine ecology progress series. Oldendorf* **13,** 99–102 (1983).

29. Araus, J. L. & Cairns, J. E. Field high-throughput phenotyping: the new crop breeding frontier. *Trends in plant science* **19,** 52–61 (2014).

30. Pereira, H. *et al.* Microplate-based high throughput screening procedure for the isolation of lipid-rich marine microalgae. *Biotechnology for biofuels* **4,** 61 (2011).

31. Kim, H. S., Weiss, T. L., Thapa, H. R., Devarenne, T. P. & Han, A. A microfluidic photobioreactor array demonstrating high-throughput screening for microalgal oil production. *Lab on a Chip* **14,** 1415–1425 (2014).

32. Radzun, K. A. *et al.* Automated nutrient screening system enables high-throughput optimisation of microalgae production conditions. *Biotechnology for biofuels* **8,** 65 (2015).

33. Furbank, R. T. & Tester, M. Phenomics–technologies to relieve the phenotyping bottleneck. *Trends in plant science* **16,** 635–644 (2011).

34. Fiorani, F. & Schurr, U. Future scenarios for plant phenotyping. *Annual review of plant biology* **64,** 267–291 (2013).

35. Pereyra-Irujo, G. A., Gasco, E. D., Peirone, L. S. & Aguirrezábal, L. A. GlyPh: a low-cost platform for phenotyping plant growth and water use. *Functional Plant Biology* **39,** 905–913 (2012).

36. Daniel K, F. & Peter J, G. Open-source hardware is a low-cost alternative for scientific instrumentation and research. *Modern instrumentation* **2012** (2012).

37. Blankenship, R. E. *Molecular mechanisms of photosynthesis* (John Wiley & Sons, 2014).

38. Whatley, F., Tagawa, K. & Arnon, D. I. Separation of the light and dark reactions in electron transfer during photosynthesis. *Proceedings of the National Academy of Sciences of the United States of America* **49,** 266 (1963).

39. Lodish, H. *et al.* in *Molecular Cell Biology. 4th edition* (WH Freeman, 2000).

40. Van Grondelle, R., Dekker, J. P., Gillbro, T. & Sundstrom, V. Energy transfer and trapping in photosynthesis. *Biochimica et Biophysica Acta (BBA)-Bioenergetics* **1187,** 1–65 (1994).

41. Hemelrijk, P. W., Kwa, S. L., van Grondelle, R. & Dekker, J. P. Spectroscopic properties of LHC-II, the main light-harvesting chlorophyll a/b protein complex from chloroplast membranes. *Biochimica et Biophysica Acta (BBA)-Bioenergetics* **1098,** 159–166 (1992).

42. Richmond, A. *Handbook of microalgal culture: biotechnology and applied phycology* (John Wiley & Sons, 2008).

43. Zigmantas, D., Hiller, R. G., Sundström, V. & Polivka, T. Carotenoid to chlorophyll energy transfer in the peridinin–chlorophyll-a–protein complex involves an intramolecular charge transfer state. *Proceedings of the National Academy of Sciences* **99,** 16760–16765 (2002).

44. Edge, R. & Truscott, T. G. in *The photochemistry of carotenoids* 223–234 (Springer, 1999).

45. Jackson, C., Clayden, S. & Reyes-Prieto, A. The Glaucophyta: the blue-green plants in a nutshell. *Acta Societatis Botanicorum Poloniae* **84** (2015).

46. Tamary, E. *et al.* Structural and functional alterations of cyanobacterial phycobilisomes induced by high-light stress. *Biochimica et Biophysica Acta (BBA)-Bioenergetics* **1817,** 319–327 (2012).

47. MacColl, R. Cyanobacterial phycobilisomes. *Journal of structural biology* **124,** 311–334 (1998).

48. Osmond, B., Chow, W. S., Pogson, B. J. & Robinson, S. A. Probing functional and optical cross-sections of PSII in leaves during state transitions using fast repetition rate light induced fluorescence transients. *Functional Plant Biology* **46,** 567–583 (2019).

49. Mullineaux, C. W. & Allen, J. F. State 1-State 2 transitions in the cyanobacterium Synechococcus 6301 are controlled by the redox state of electron carriers between Photosystems I and II. *Photosynthesis research* **23,** 297–311 (1990).

50. Wobbe, L., Bassi, R. & Kruse, O. Multi-level light capture control in plants and green algae. *Trends in Plant Science* **21,** 55–68 (2016).

51. Joliot, P. & Johnson, G. N. Regulation of cyclic and linear electron flow in higher plants. *Proceedings of the National Academy of Sciences* **108,** 13317–13322 (2011).

52. Takizawa, K., Cruz, J. A., Kanazawa, A. & Kramer, D. M. The thylakoid proton motive force in vivo. Quantitative, non-invasive probes, energetics, and regulatory consequences of light-induced pmf. *Biochimica et Biophysica Acta (BBA)-Bioenergetics* **1767,** 1233–1244 (2007).

53. Cruz, J. A. *et al.* Plasticity in light reactions of photosynthesis for energy production and photoprotection. *Journal of experimental botany* **56,** 395–406 (2005).

54. Barber, J. & Archer, M. P680, the primary electron donor of photosystem II. *Journal of Photochemistry and Photobiology A: Chemistry* **142,** 97–106 (2001).

55. Allakhverdiev, S. I. *et al.* Redox potentials of primary electron acceptor quinone molecule (QA)- and conserved energetics of photosystem II in cyanobacteria with chlorophyll a and chlorophyll d. *Proceedings of the National Academy of Sciences* **108,** 8054–8058 (2011).

56. Kramer, D. M., Avenson, T. J. & Edwards, G. E. Dynamic flexibility in the light reactions of photosynthesis governed by both electron and proton transfer reactions. *Trends in plant science* **9,** 349–357 (2004).

57. Bates, H., Zavafer, A., Szabó, M. & Ralph, P. J. A guide to Open-JIP, a low-cost open-source chlorophyll fluorometer. *Photosynthesis research* **142,** 361–368 (2019).

58. Duysens, L. & Sweers, H. in *Jap. Soc. Plant Physiol.* 353–372 (University of Tokyo Press Tokyo, 1963).

59. Maxwell, K. & Johnson, G. N. Chlorophyll fluorescence—a practical guide. *Journal of experimental botany* **51,** 659–668 (2000).

60. Müller, P., Li, X.-P. & Niyogi, K. K. Non-photochemical quenching. A response to excess light energy. *Plant physiology* **125,** 1558–1566 (2001).

61. Schreiber, U., Klughammer, C. & Kolbowski, J. Assessment of wavelength-dependent parameters of photosynthetic electron transport with a new type of multi-color PAM chlorophyll fluorometer. *Photosynthesis research* **113,** 127–144 (2012).

62. Strasser, R. J. & Govindjee. in *Regulation of chloroplast biogenesis* 423–426 (Springer, 1992).

63. Vredenberg, W. J. System analysis and photoelectrochemical control of chlorophyll fluorescence in terms of trapping models of photosystem II: a challenging view, 133–172 (2004).

64. Stirbet, A. & Govindjee. On the relation between the Kautsky effect (chlorophyll a fluorescence induction) and photosystem II: basics and applications of the OJIP fluorescence transient. *Journal of Photochemistry and Photobiology B: Biology* **104,** 236–257 (2011).

65. Kromkamp, J. C. & Forster, R. M. The use of variable fluorescence measurements in aquatic ecosystems: differences between multiple and single turnover measuring protocols and suggested terminology. *European Journal of Phycology* **38,** 103–112 (2003).

66. Nagy, V. *et al.* Stimulatory effect of ascorbate, the alternative electron donor of photosystem II, on the hydrogen production of sulphur-deprived Chlamydomonas reinhardtii. *international journal of hydrogen energy* **37,** 8864–8871 (2012).

67. Tsimilli-Michael, M. & Strasser, R. J. in *Piriformospora indica* 173–190 (Springer, 2013).

68. Strasser, R. J., Tsimilli-Michael, M. & Srivastava, A. in *Chlorophyll a fluorescence* 321–362 (Springer, 2004).

69. Strasser, R. The grouping model of plant photosynthesis. *Chloroplast development,* 513–542 (1978).

70. Osmond, B. *et al.* Relative functional and optical absorption cross-sections of PSII and other photosynthetic parameters monitored in situ, at a distance with a time resolution of a few seconds, using a prototype light induced fluorescence transient (LIFT) device. *Functional Plant Biology* **44,** 985–1006 (2017).

71. Szabó, M. *et al.* Photosynthetic acclimation of Nannochloropsis oculata investigated by multi-wavelength chlorophyll fluorescence analysis. *Bioresource technology* **167,** 521–529 (2014).

72. Schreiber, U. in *Chlorophyll a fluorescence* 279–319 (Springer, 2004).

73. Rascher, U., Liebig, M. & Lüttge, U. Evaluation of instant light-response curves of chlorophyll fluorescence parameters obtained with a portable chlorophyll fluorometer on site in the field. *Plant, Cell & Environment* **23,** 1397–1405 (2000).

74. Genty, B., Briantais, J.-M. & Baker, N. R. The relationship between the quantum yield of photosynthetic electron transport and quenching of chlorophyll fluorescence. *Biochimica et Biophysica Acta (BBA)-General Subjects* **990,** 87–92 (1989).

75. Schreiber, U., Bilger, W. & Neubauer, C. Chlorophyll fluorescence as a nonintrusive indicator for rapid assessment of in vivo photosynthesis, 49–70 (1995).

76. Björkman, O. & Demmig, B. Photon yield of O 2 evolution and chlorophyll fluorescence characteristics at 77 K among vascular plants of diverse origins. *Planta* **170,** 489–504 (1987).

77. Lichtenthaler, H. K. in *Applications of chlorophyll fluorescence in photosynthesis research, stress physiology, hydrobiology and remote sensing* 129–142 (Springer, 1988).

78. Kitajima, M. & Butler, W. Quenching of chlorophyll fluorescence and primary photochemistry in chloroplasts by dibromothymoquinone. *Biochimica et Biophysica Acta (BBA)-Bioenergetics* **376,** 105–115 (1975).

79. Strasser, B. J. Donor side capacity of photosystem II probed by chlorophyll a fluorescence transients. *Photosynthesis Research* **52,** 147–155 (1997).

80. Strasser, R. J., Srivastava, A. & Tsimilli-Michael, M. The fluorescence transient as a tool to characterize and screen photosynthetic samples. *Probing photosynthesis: mechanisms, regulation and adaptation,* 445–483 (2000).

81. Strasser Bruno J amd Strasser, R. J. Measuring fast fluorescence transients to address environmental questions; the JIP-test. *Photosynthesis: from light to biosphere,* 977–980 (1995).

82. Bolch, C. J. & Blackburn, S. I. Isolation and purification of Australian isolates of the toxic cyanobacteriumMicrocystis aeruginosa Kütz. *Journal of Applied Phycology* **8,** 5–13 (1996).

83. Moore, L. R. *et al.* Culturing the marine cyanobacterium Prochlorococcus. *Limnology and Oceanography: Methods* **5,** 353–362 (2007).

84. Tóth, S. Z., Puthur, J. T., Nagy, V. & Garab, G. Experimental evidence for ascorbate-dependent electron transport in leaves with inactive oxygen-evolving complexes. *Plant physiology* **149,** 1568–1578 (2009).

85. Schansker, G., Tóth, S. Z., Kovács, L., Holzwarth, A. R. & Garab, G. Evidence for a fluorescence yield change driven by a light-induced conformational change within photosystem II during the fast chlorophyll a fluorescence rise. *Biochimica et Biophysica Acta (BBA)-Bioenergetics* **1807,** 1032–1043 (2011).

86. Hoadley, K. D. & Warner, M. E. Use of Open Source Hardware and Software Platforms to Quantify Spectrally Dependent Differences in Photochemical Efficiency and Functional Absorption Cross Section within the Dinoflagellate Symbiodinium spp. *Frontiers in Marine Science* **4,** 365 (2017).

87. Leeuw, T., Boss, E. S. & Wright, D. L. In situ measurements of phytoplankton fluorescence using low cost electronics. *Sensors* **13,** 7872–7883 (2013).

88. Teramoto, H., Nakamori, A., Minagawa, J. & Ono, T.-a. Light-intensity-dependent expression of Lhc gene family encoding light-harvesting chlorophyll-a/b proteins of photosystem II in Chlamydomonas reinhardtii. *Plant Physiology* **130,** 325–333 (2002).

89. Benemann, J. R. CO2 mitigation with microalgae systems. *Energy conversion and management* **38,** S475–S479 (1997).

90. Da Silva Vaz, B., Moreira, J. B., de Morais, M. G. & Costa, J. A. V. Microalgae as a new source of bioactive compounds in food supplements. *Current Opinion in Food Science* **7,** 73–77 (2016).

91. Draaisma, R. B. *et al.* Food commodities from microalgae. *Current opinion in biotechnology* **24,** 169–177 (2013).

92. Mata, T. M., Martins, A. A. & Caetano, N. S. Microalgae for biodiesel production and other applications: a review. *Renewable and sustainable energy reviews* **14,** 217–232 (2010).

93. Borowitzka, M. A. Microalgae as sources of pharmaceuticals and other biologically active compounds. *Journal of applied phycology* **7,** 3–15 (1995).

94. Han, F. *et al.* Optimization and lipid production enhancement of microalgae culture by efficiently changing the conditions along with the growth-state. *Energy Conversion and Management* **90,** 315–322 (2015).

95. Agrawal, A. A. Phenotypic plasticity in the interactions and evolution of species. *Science* **294,** 321–326 (2001).

96. Petrou, K. & Ralph, P. Photosynthesis and net primary productivity in three Antarctic diatoms: possible significance for their distribution in the Antarctic marine ecosystem. *Marine Ecology Progress Series* **437,** 27–40 (2011).

97. Suh, I. S. & Lee, C.-G. Photobioreactor engineering: design and performance. *Biotechnology and bioprocess engineering* **8,** 313 (2003).

98. Singh, R. & Sharma, S. Development of suitable photobioreactor for algae production–A review. *Renewable and Sustainable Energy Reviews* **16,** 2347–2353 (2012).

99. Cruz, J. A. *et al.* Dynamic environmental photosynthetic imaging reveals emergent phenotypes. *Cell Systems* **2,** 365–377 (2016).

100. Lucker, B. F., Hall, C. C., Zegarac, R. & Kramer, D. M. The environmental photobioreactor (ePBR): An algal culturing platform for simulating dynamic natural environments. *Algal research* **6,** 242–249 (2014).

101. Nedbal, L., Trtílek, M., Červený, J., Komárek, O. & Pakrasi, H. B. A photobioreactor system for precision cultivation of photoautotrophic microorganisms and for high-content analysis of suspension dynamics. *Biotechnology and Bioengineering* **100,** 902–910 (2008).

102. Bates, H., Zavafer, A., Szabó, M. & Ralph, P. J. *Phenobottle v0.1* version v0.1. Mar. 2020. `https://doi.org/10.5281/zenodo.3728645`.

103. Schulze, P. S., Barreira, L. A., Pereira, H. G., Perales, J. A. & Varela, J. C. Light emitting diodes (LEDs) applied to microalgal production. *Trends in biotechnology* **32,** 422–430 (2014).

104. Glemser, M. *et al.* Application of light-emitting diodes (LEDs) in cultivation of phototrophic microalgae: current state and perspectives. *Applied microbiology and biotechnology* **100,** 1077–1088 (2016).

105. Wood, A. M., Everroad, R. & Wingard, L. Measuring growth rates in microalgal cultures. *Algal culturing techniques* **18,** 269–288 (2005).

106. Beutler, M. *et al.* A fluorometric method for the differentiation of algal populations in vivo and in situ. *Photosynthesis research* **72,** 39–53 (2002).

107. Goltsev, V. *et al.* Variable chlorophyll fluorescence and its use for assessing physiological condition of plant photosynthetic apparatus. *Russian journal of plant physiology* **63,** 869–893 (2016).

108. Blair, M. F., Kokabian, B. & Gude, V. G. Light and growth medium effect on Chlorella vulgaris biomass production. *Journal of environmental chemical engineering* **2,** 665–674 (2014).

109. Lam, M. K. & Lee, K. T. Effect of carbon source towards the growth of Chlorella vulgaris for CO2 bio-mitigation and biodiesel production. *International Journal of Greenhouse Gas Control* **14,** 169–176 (2013).

110. Sakarika, M. & Kornaros, M. Kinetics of growth and lipids accumulation in Chlorella vulgaris during batch heterotrophic cultivation: Effect of different nutrient limitation strategies. *Bioresource Technology* **243,** 356–365 (2017).

111. Oukarroum, A. Change in photosystem II photochemistry during algal growth phases of Chlorella vulgaris and Scenedesmus obliquus. *Current microbiology* **72,** 692–699 (2016).

112. Tessmer, O. L., Kramer, D. M. & Chen, J. *OLIVER: A Tool for Visual Data Analysis on Longitudinal Plant Phenomics Data* in *2018 IEEE International Conference on Bioinformatics and Biomedicine (BIBM)* (2018), 510–517.

113. Sorek, M., Yacobi, Y. Z., Roopin, M., Berman-Frank, I. & Levy, O. Photosynthetic circadian rhythmicity patterns of Symbiodium, the coral endosymbiotic algae. *Proceedings of the Royal Society B: Biological Sciences* **280,** 20122942 (2013).

114. Wang, B., Lan, C. Q. & Horsman, M. Closed photobioreactors for production of microalgal biomasses. *Biotechnology advances* **30,** 904–912 (2012).

115. Fabris, M. *et al.* Emerging Technologies in Algal Biotechnology: Toward the Establishment of a Sustainable, Algae-Based Bioeconomy. *Frontiers in Plant Science* **11** (2020).

116. Ahmad, M. T., Shariff, M., Md. Yusoff, F., Goh, Y. M. & Banerjee, S. Applications of microalga Chlorella vulgaris in aquaculture. *Reviews in Aquaculture* **12,** 328–346 (2020).

117. Maity, J. P., Bundschuh, J., Chen, C.-Y. & Bhattacharya, P. Microalgae for third generation biofuel production, mitigation of greenhouse gas emissions and wastewater treatment: Present and future perspectives–A mini review. *Energy* **78,** 104–113 (2014).

118. Sforza, E., Simionato, D., Giacometti, G. M., Bertucco, A. & Morosinotto, T. Adjusted light and dark cycles can optimize photosynthetic efficiency in algae growing in photobioreactors. *PloS one* **7,** e38975 (2012).

119. Shin, W.-S., Lee, B., Jeong, B.-r., Chang, Y. K. & Kwon, J.-H. Truncated light-harvesting chlorophyll antenna size in Chlorella vulgaris improves biomass productivity. *Journal of Applied Phycology* **28,** 3193–3202 (2016).

120. Stirbet, A., Riznichenko, G. Y., Rubin, A., *et al.* Modeling chlorophyll a fluorescence transient: relation to photosynthesis. *Biochemistry (Moscow)* **79,** 291–323 (2014).

121. Briantais, J.-M., Vernotte, C., Picaud, M. & Krause, G. A quantitative study of the slow decline of chlorophyll a fluorescence in isolated chloroplasts. *Biochimica et Biophysica Acta (BBA)-Bioenergetics* **548,** 128–138 (1979).